



MULTI-SCALE NUCLEAR IMAGING AT THE EIC

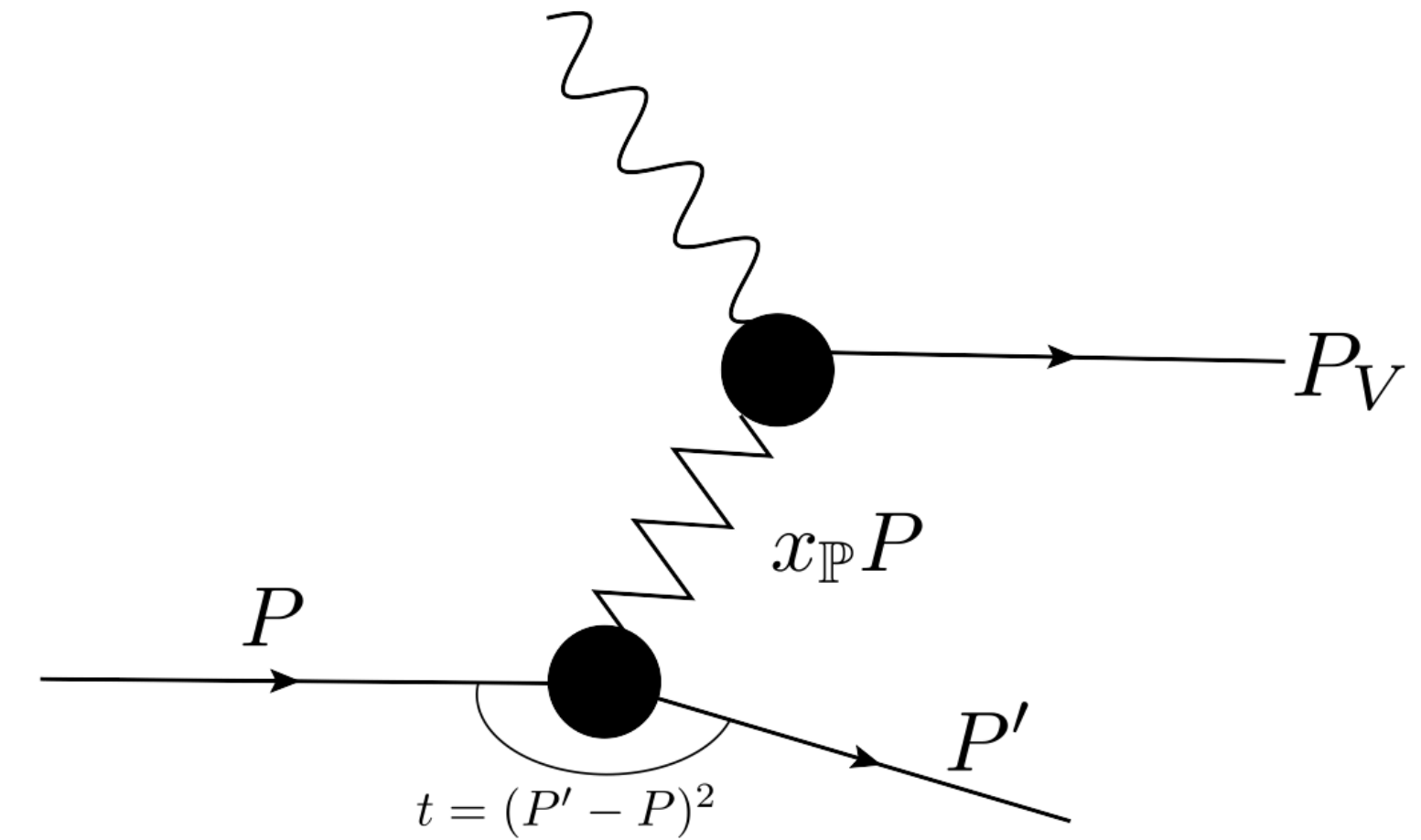
BJÖRN SCHENKE, BROOKHAVEN NATIONAL LABORATORY

Electron-Nuclei Interaction at the EIC
CFNS SBU
07/07/2023

Diffractive vector meson production

— Coherent diffraction:
$$\frac{d\sigma^{\gamma^*p \rightarrow Vp}}{dt} = \frac{1}{16\pi} \left| \left\langle A^{\gamma^*p \rightarrow Vp} \left(x_P, Q^2, \vec{\Delta} \right) \right\rangle \right|^2$$

sensitive to the average size of the target



— Incoherent diffraction:
$$\frac{d\sigma^{\gamma^*p \rightarrow Vp^*}}{dt} = \frac{1}{16\pi} \left(\left\langle \left| A^{\gamma^*p \rightarrow Vp} \left(x_P, Q^2, \vec{\Delta} \right) \right|^2 \right\rangle - \left| \left\langle A^{\gamma^*p \rightarrow Vp} \left(x_P, Q^2, \vec{\Delta} \right) \right\rangle \right|^2 \right)$$

sensitive to fluctuations (including geometric ones)

H. Kowalski, L. Motyka, G. Watt, Phys.Rev. D 74 (2006) 074016

A. Caldwell, H. Kowalski, EDS 09, 190-192, e-Print: 0909.1254 [hep-ph]

M. L. Good and W. D. Walker, Phys. Rev. 120 (1960) 1857

H. I. Miettinen and J. Pumplin, Phys. Rev. D18 (1978) 1696

Y. V. Kovchegov and L. D. McLerran, Phys. Rev. D60 (1999) 054025

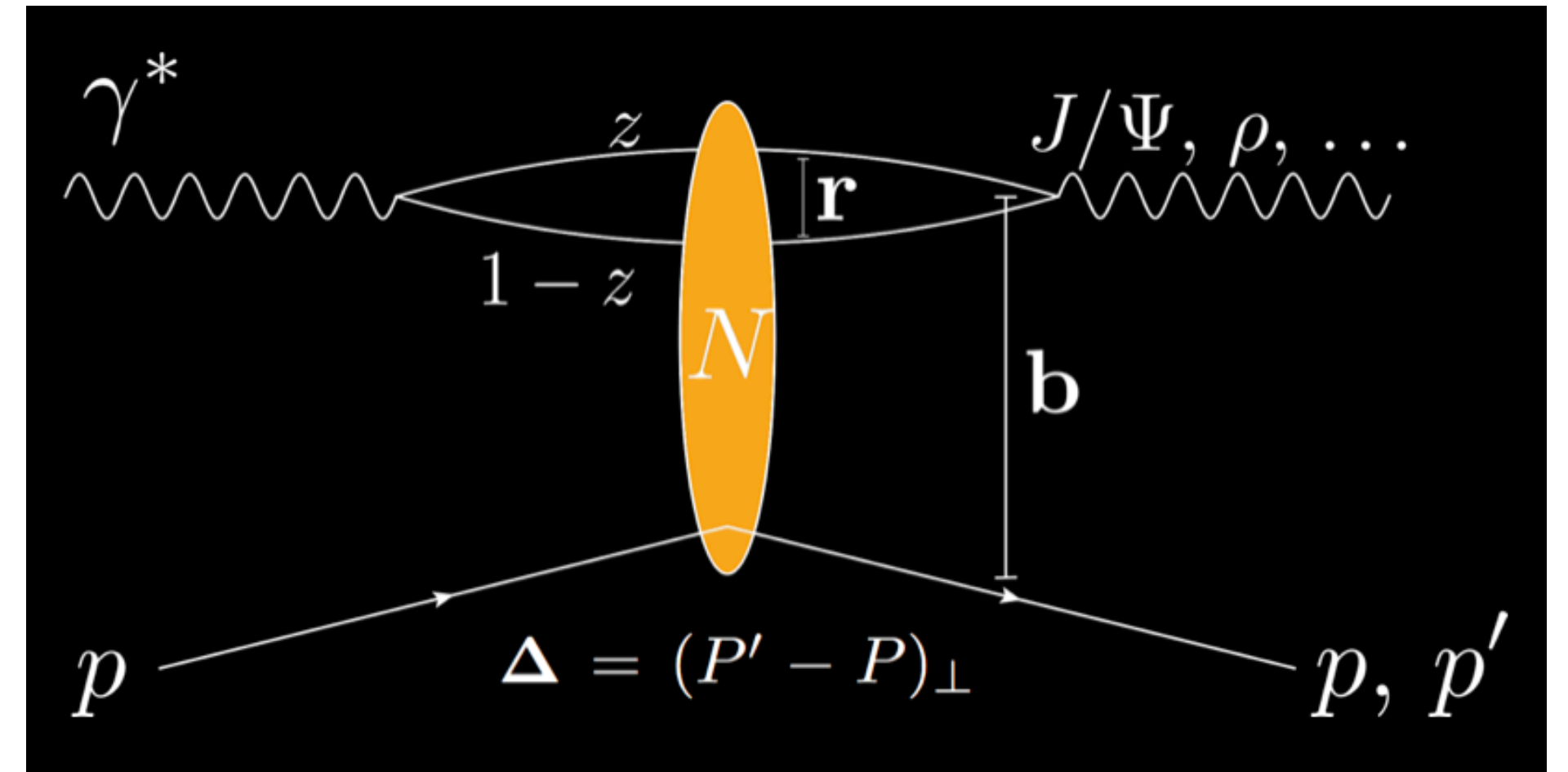
A. Kovner and U. A. Wiedemann, Phys. Rev. D64 (2001) 114002

Dipole picture: Scattering amplitude

H. Mäntysaari, B. Schenke, Phys. Rev. Lett. 117 (2016) 052301; Phys.Rev. D94 (2016) 034042

High energy factorization:

- $\gamma^* \rightarrow q\bar{q} : \psi^\gamma(r, Q^2, z)$
- $q\bar{q}$ dipole scatters with amplitude N
- $q\bar{q} \rightarrow V : \psi^V(r, Q^2, z)$



$$A \sim \int d^2b dz d^2r \psi^* \psi^V(\vec{r}, z, Q^2) e^{-i\vec{b} \cdot \vec{\Delta}} N(\vec{r}, x, \vec{b})$$

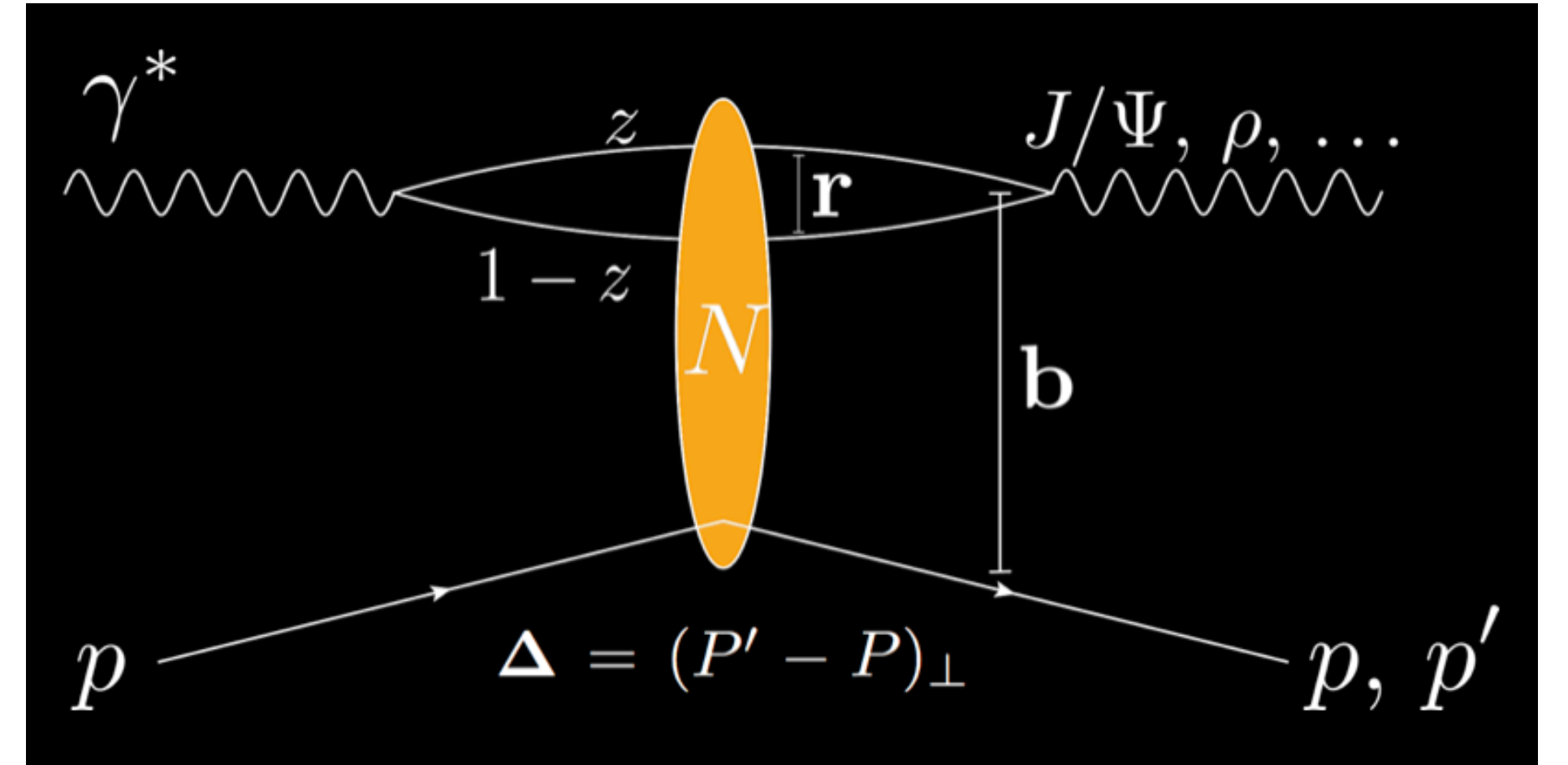
- Impact parameter \mathbf{b} is the Fourier conjugate of transverse momentum transfer $\mathbf{\Delta} \rightarrow$ Access to spatial structure ($t = -\Delta^2$)

Color glass condensate formalism

H. Mäntysaari, B. Schenke, Phys. Rev. Lett. 117 (2016) 052301; Phys.Rev. D94 (2016) 034042

Compute the Wilson lines using color charges whose correlator depends on \vec{b}_\perp

$$\langle \rho^a(\mathbf{b}_\perp) \rho^b(\mathbf{x}_\perp) \rangle = g^2 \mu^2(x, \mathbf{b}_\perp) \delta^{ab} \delta^{(2)}(\mathbf{b}_\perp - \mathbf{x}_\perp)$$



$$N(\vec{r}, x, \vec{b}) = N(\vec{x} - \vec{y}, x, (\vec{x} + \vec{y})/2) = 1 - \text{Tr}(\mathbf{V}(\vec{x}) \mathbf{V}^\dagger(\vec{y})) / N_c$$

The trace appears at the level of the amplitude, because we project on a **color singlet**

$$A \sim \int d^2b dz d^2r \psi^* \psi^V(\vec{r}, z, Q^2) e^{-i\vec{b} \cdot \vec{\Delta}} N(\vec{r}, x, \vec{b})$$

Model impact parameter dependence (proton, nucleon)

H. Mäntysaari, B. Schenke, Phys. Rev. Lett. 117 (2016) 052301; Phys.Rev. D94 (2016) 034042

1) Assume Gaussian proton shape:

$$T(\vec{b}) = T_p(\vec{b}) = \frac{1}{2\pi B_p} e^{-b^2/(2B_p)}$$

2) Assume Gaussian distributed and Gaussian shaped hot spots:

$$P(b_i) = \frac{1}{2\pi B_{qc}} e^{-b_i^2/(2B_{qc})} \quad (\text{angles uniformly distributed})$$

$$T_p(\vec{b}) = \frac{1}{N_q} \sum_{i=1}^{N_q} T_q(\vec{b} - \vec{b}_i) \quad \text{with } N_q \text{ hot spots;} \quad T_q(\vec{b}) = \frac{1}{2\pi B_q} e^{-b^2/(2B_q)}$$

Diffractive J/ψ production in e+p at HERA

Nucleon parameters $B_{q'}$, $B_{qc'}$ can be constrained by e+p scattering data from HERA

Exclusive diffractive J/ψ production in e+p:

Incoherent x-sec sensitive to fluctuations

H. Mäntysaari, B. Schenke, Phys. Rev. Lett. 117 (2016) 052301

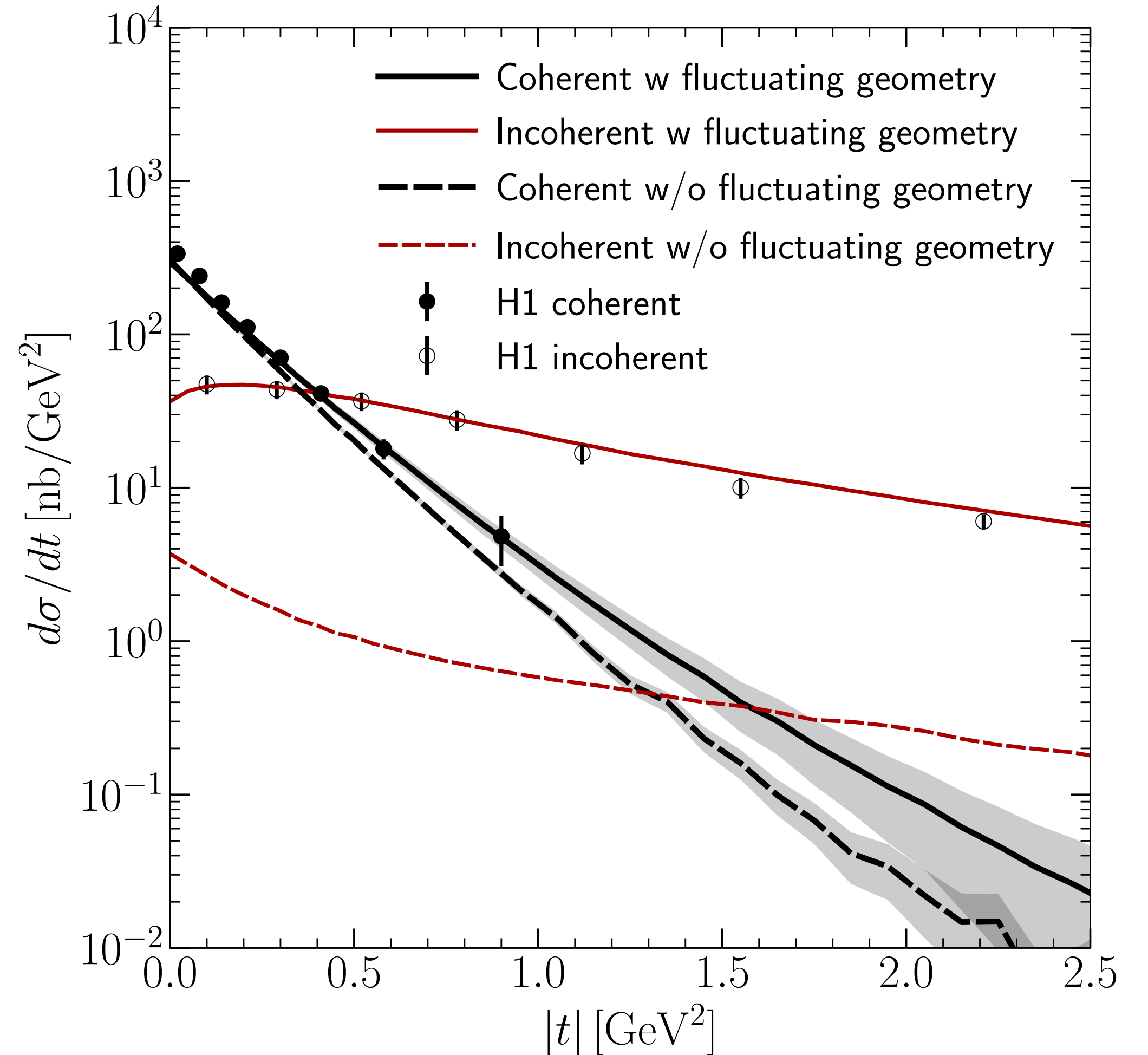
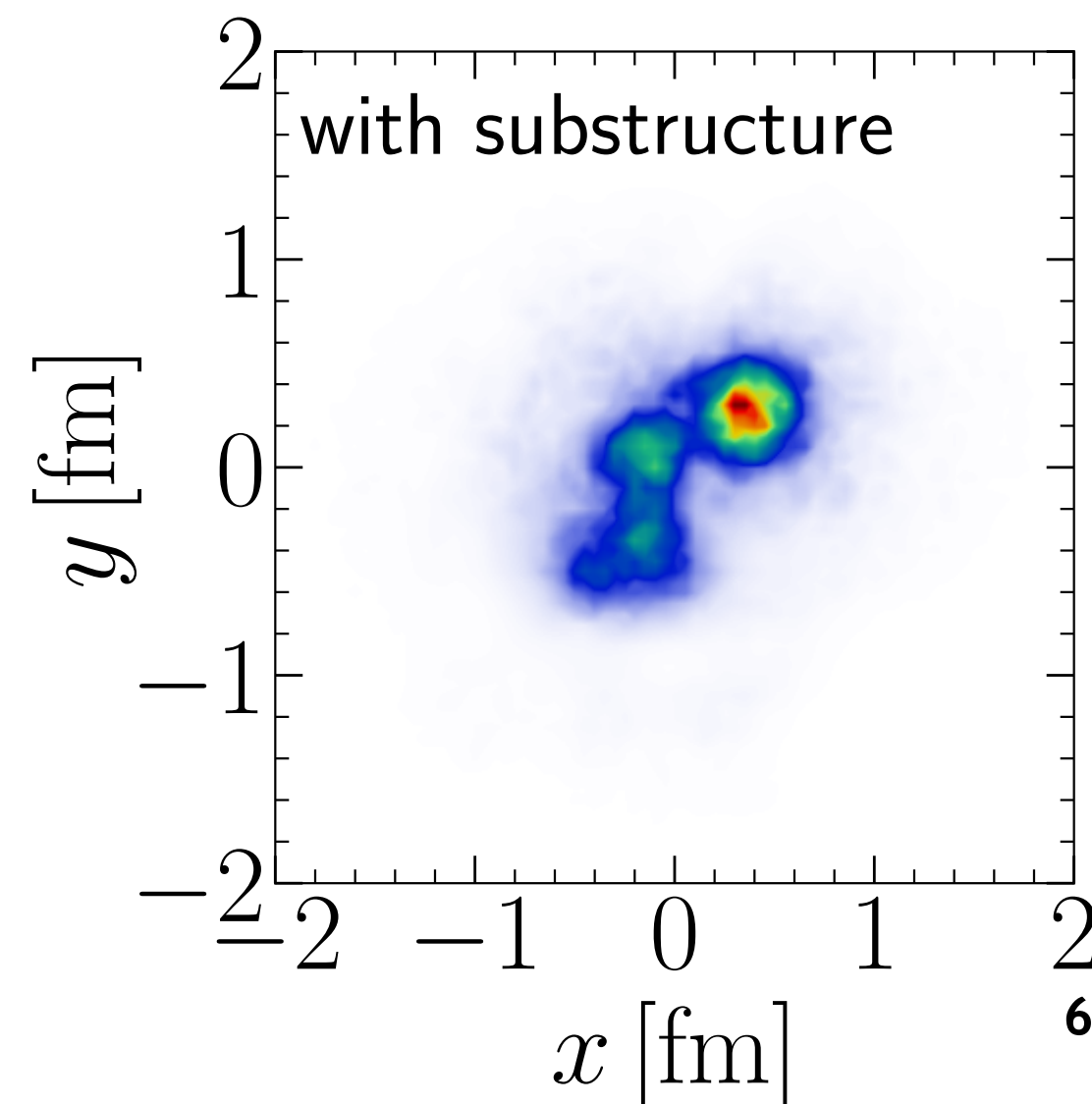
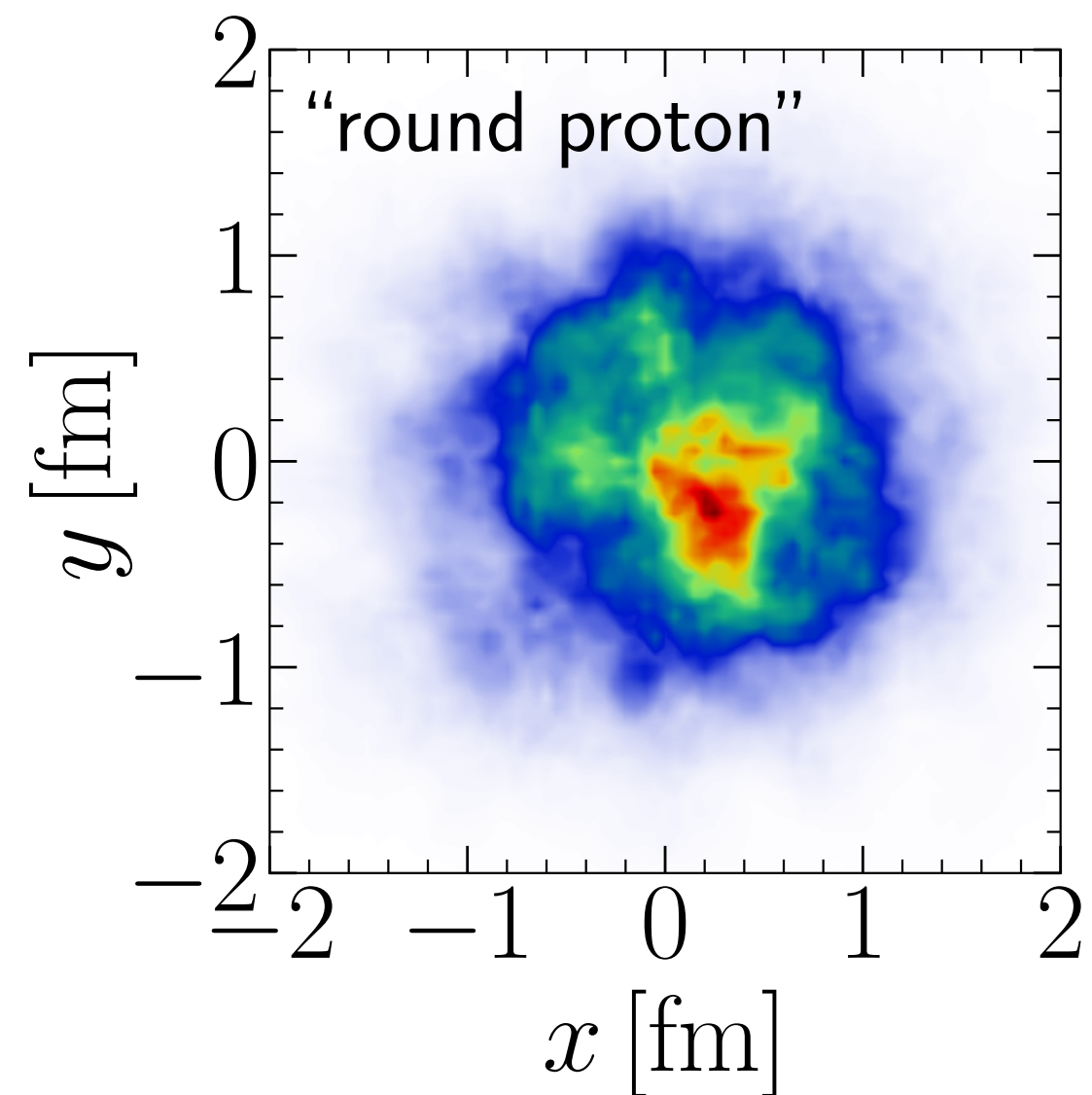
Phys.Rev. D94 (2016) 034042

also see:

S. Schlichting, B. Schenke, Phys.Lett. B739 (2014) 313-319

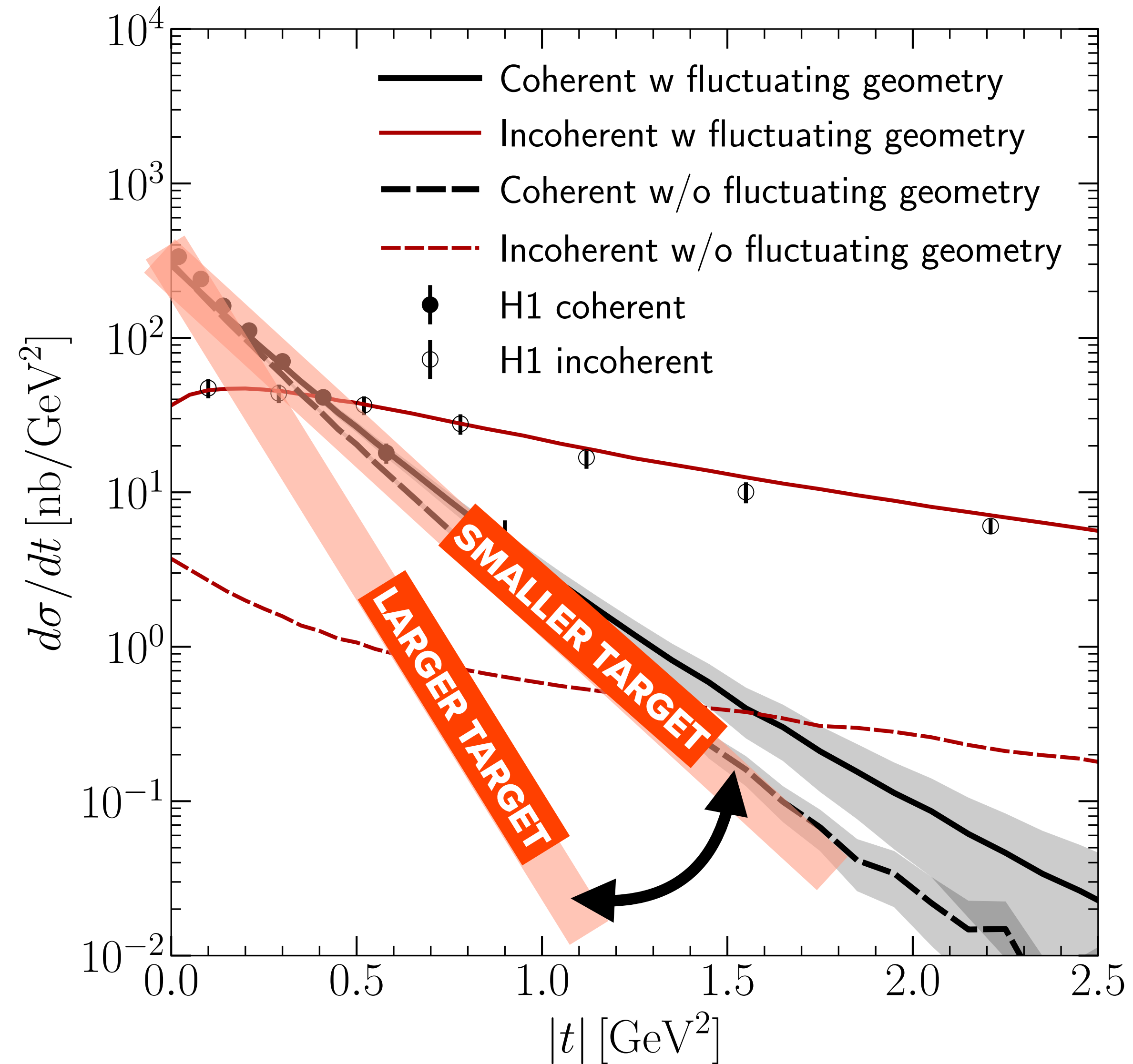
H. Mäntysaari, Rep. Prog. Phys. 83 082201 (2020)

B. Schenke, Rep. Prog. Phys. 84 082301 (2021)



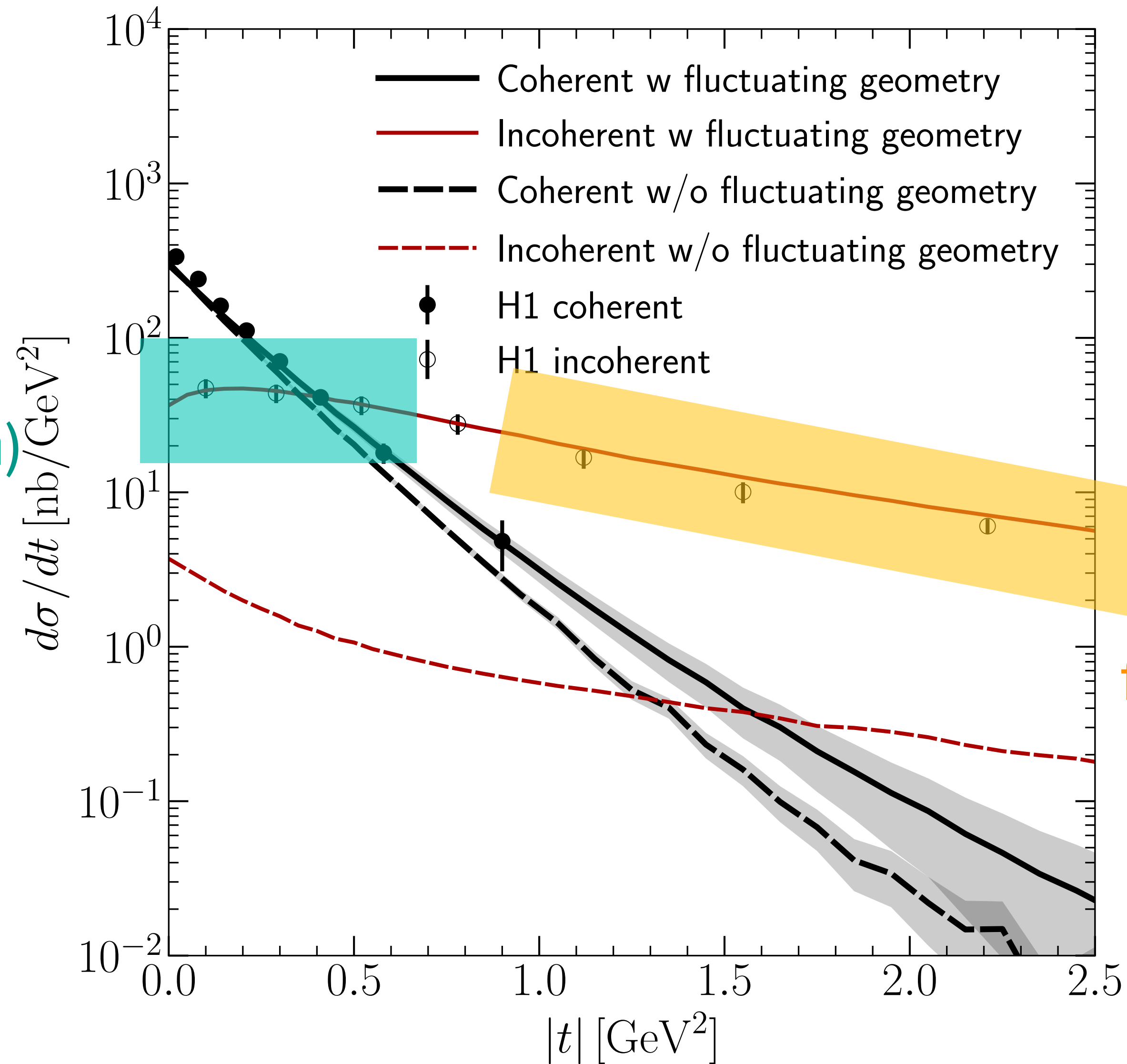
H1 Collaboration, Eur. Phys. J. C73 (2013) no. 6 2466

Information in the diffractive cross sections



Information in the diffractive cross sections

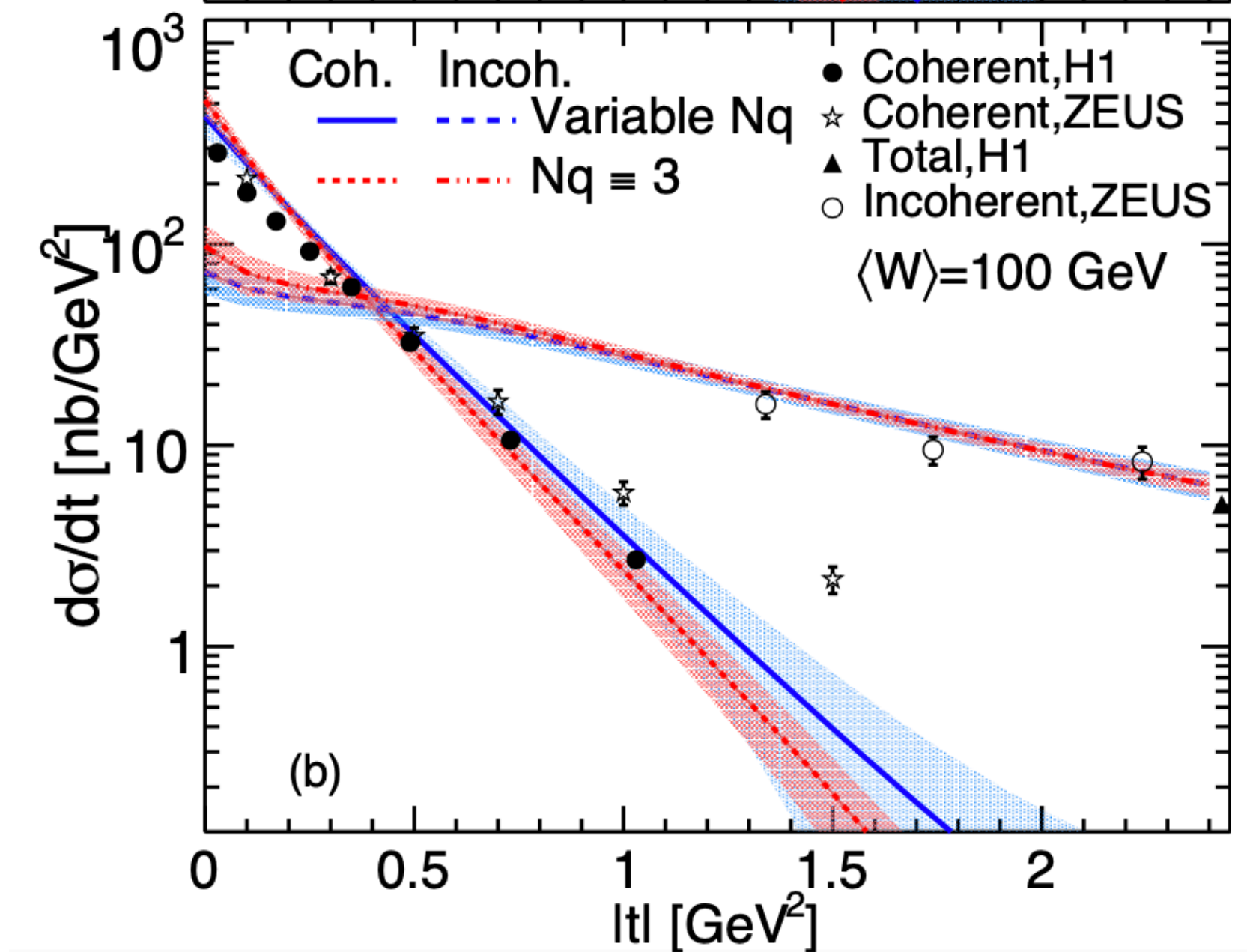
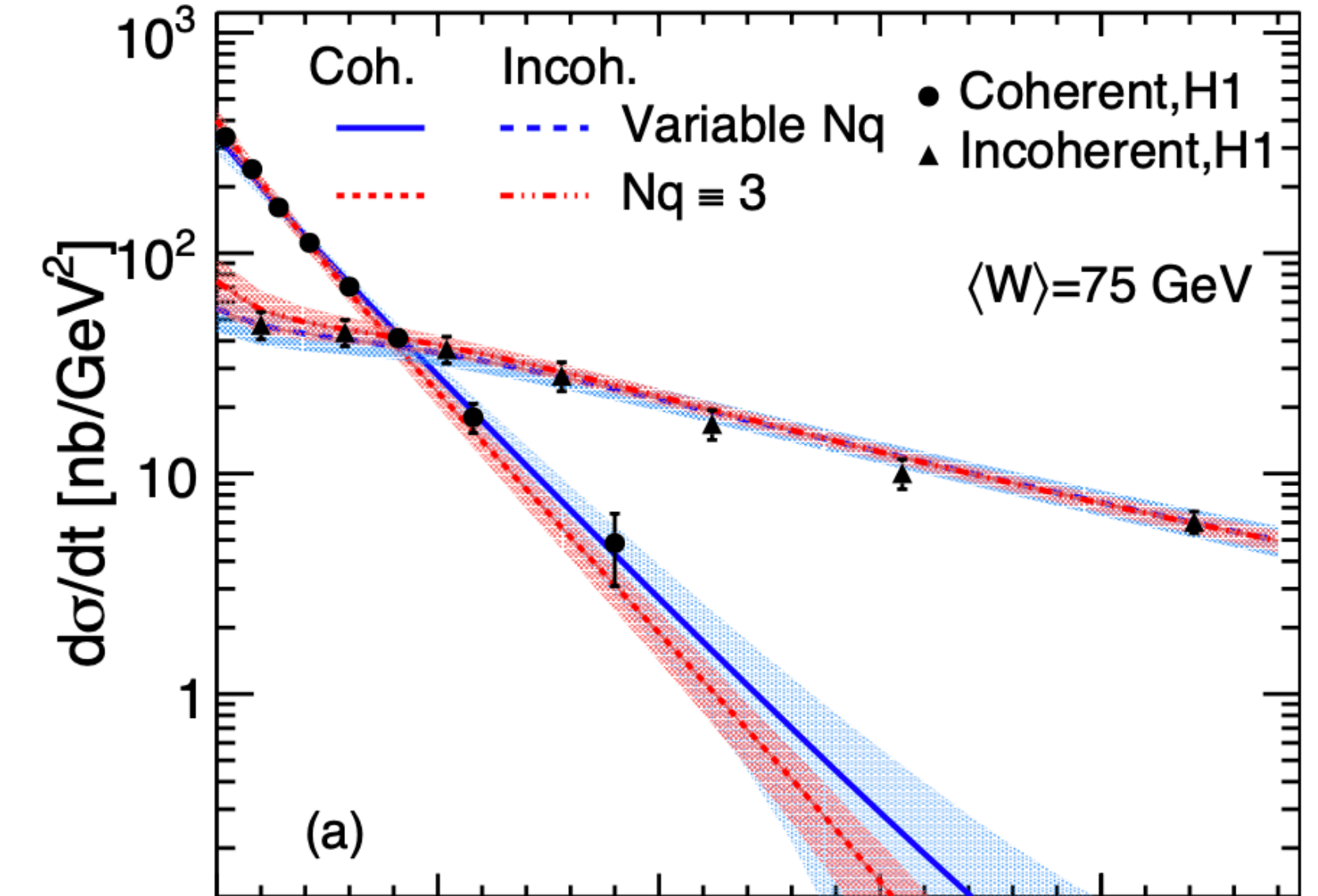
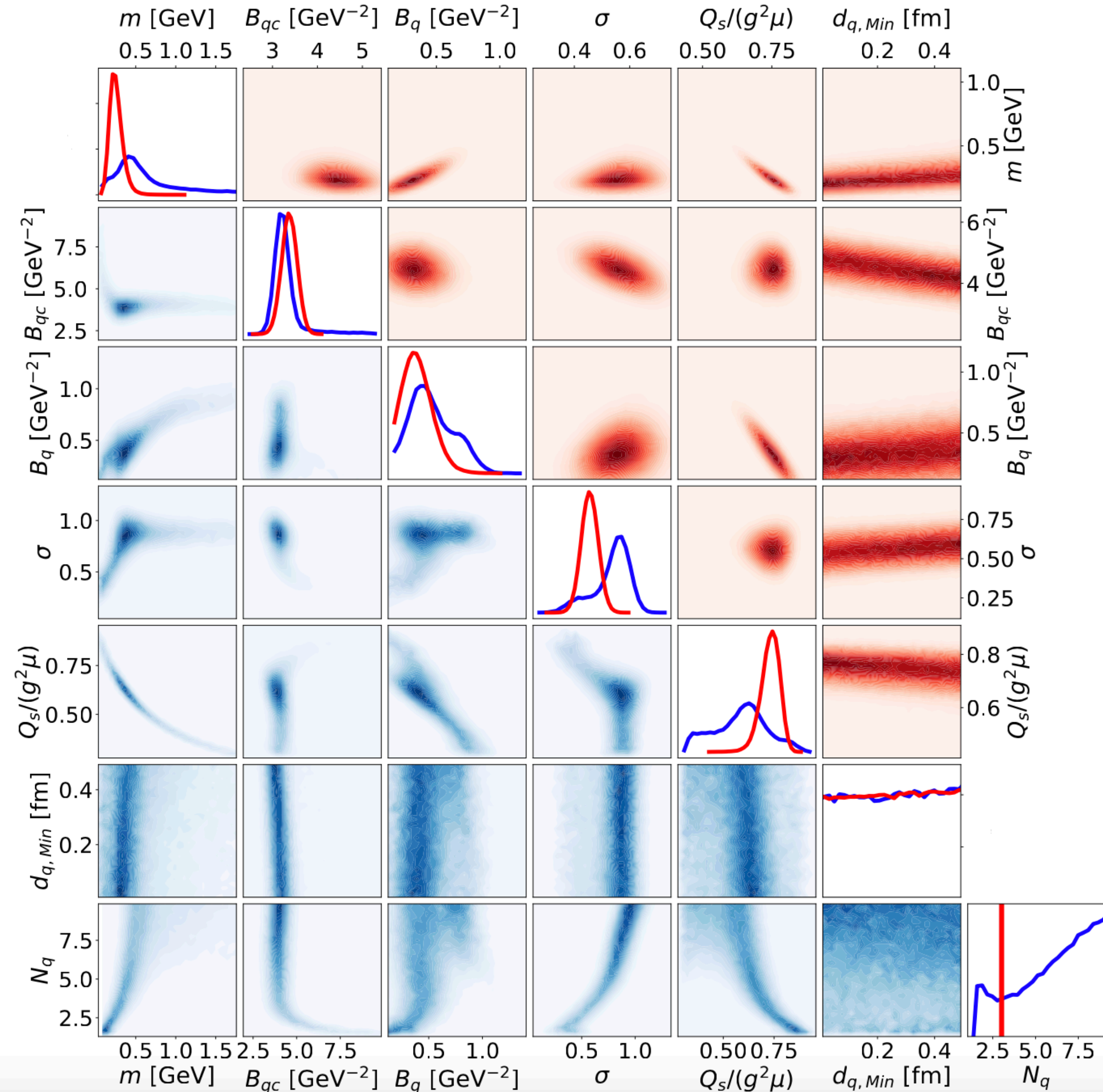
larger scale
fluctuations (>0.2 fm)



short scale
fluctuations (<0.2 fm)

Extracting parameters using Bayesian inference

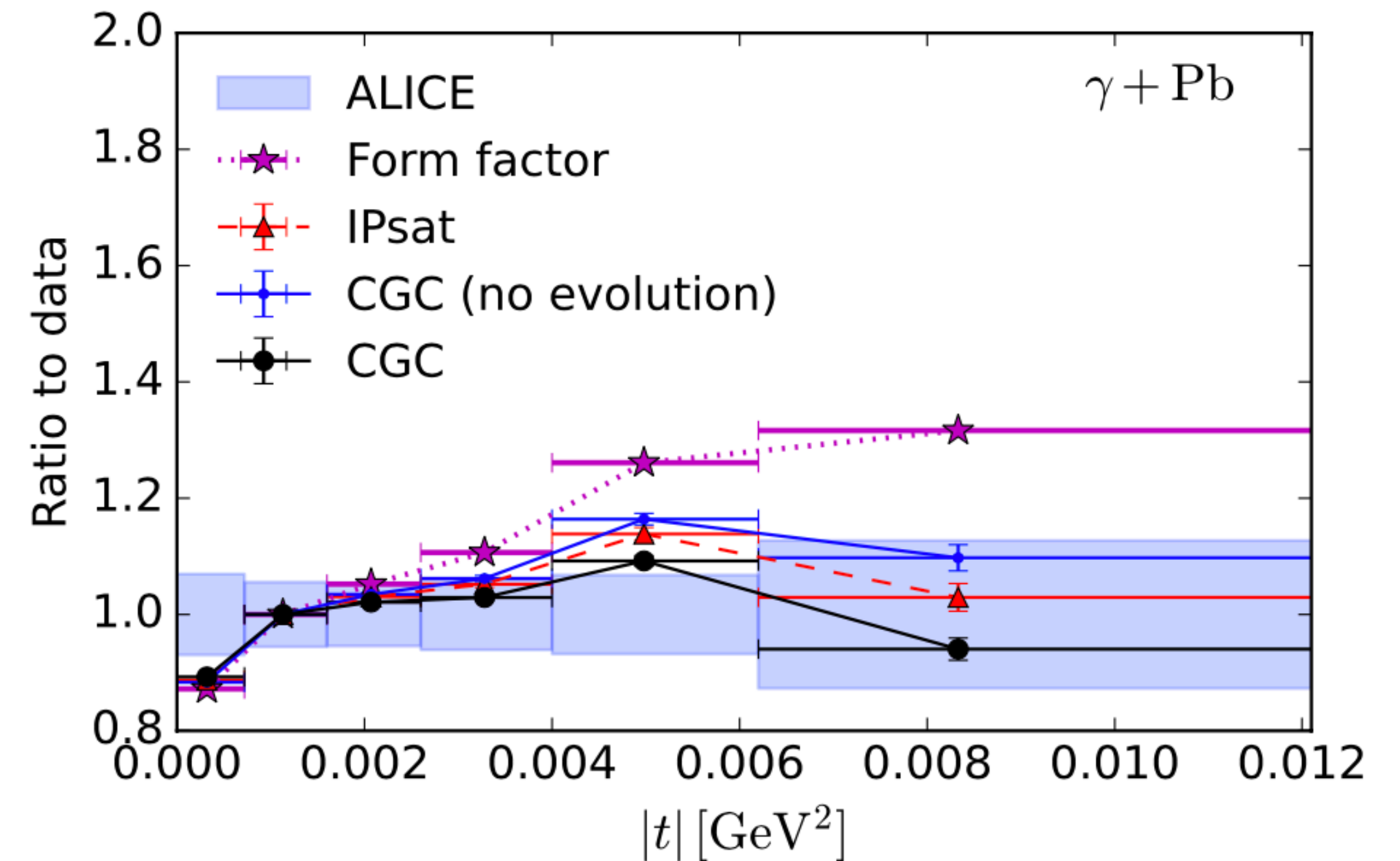
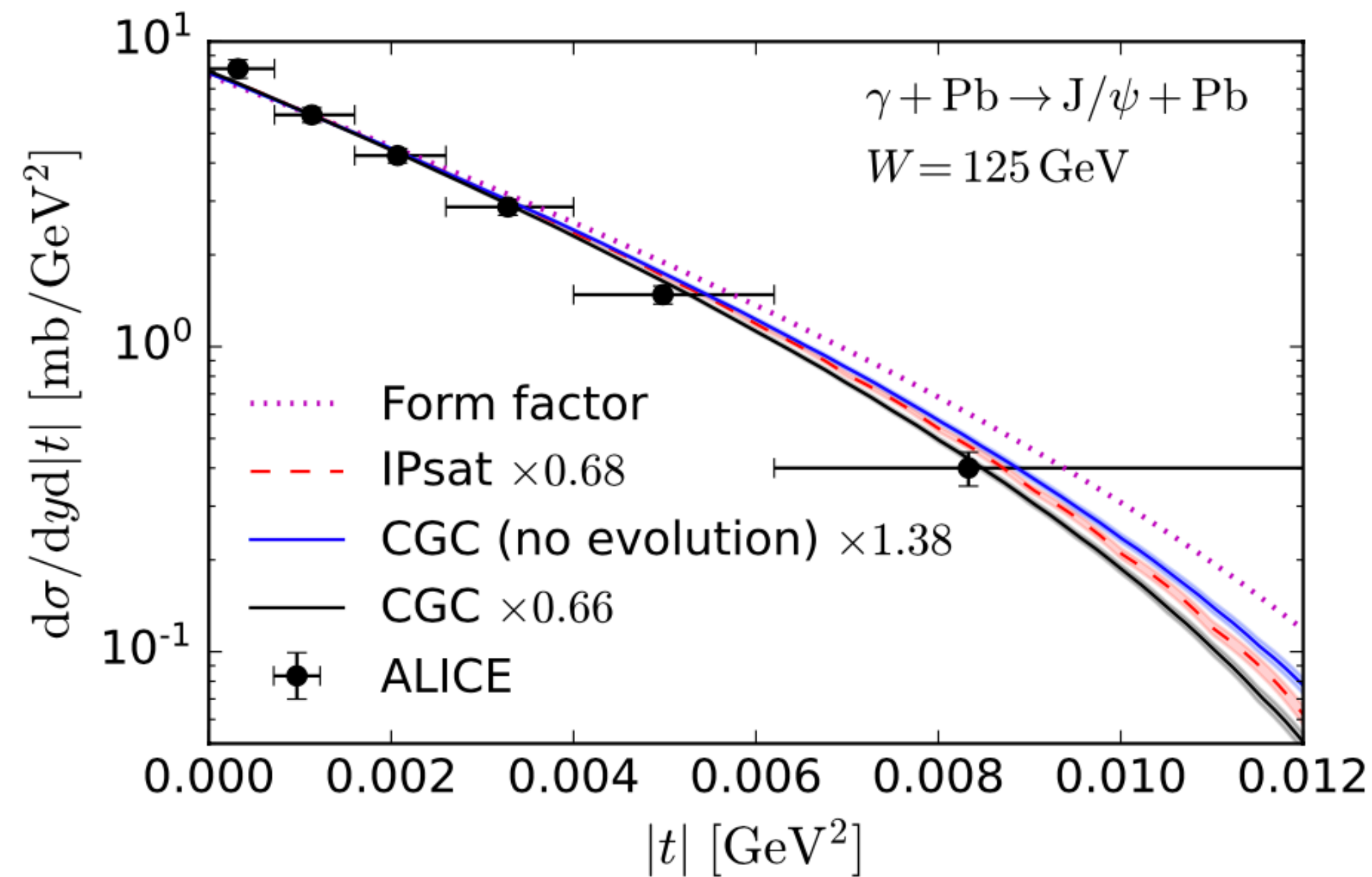
H. Mäntysaari, B. Schenke, C. Shen, W. Zhao, Phys.Lett.B 833 (2022) 137348



UPCs: γ +Pb measurement - Role of saturation effects

H. Mäntysaari, F. Salazar, B. Schenke, *Phys.Rev.D* 106 (2022) 7, 074019

Here, ALICE removed interference and photon k_T effects to get the γ +Pb cross section



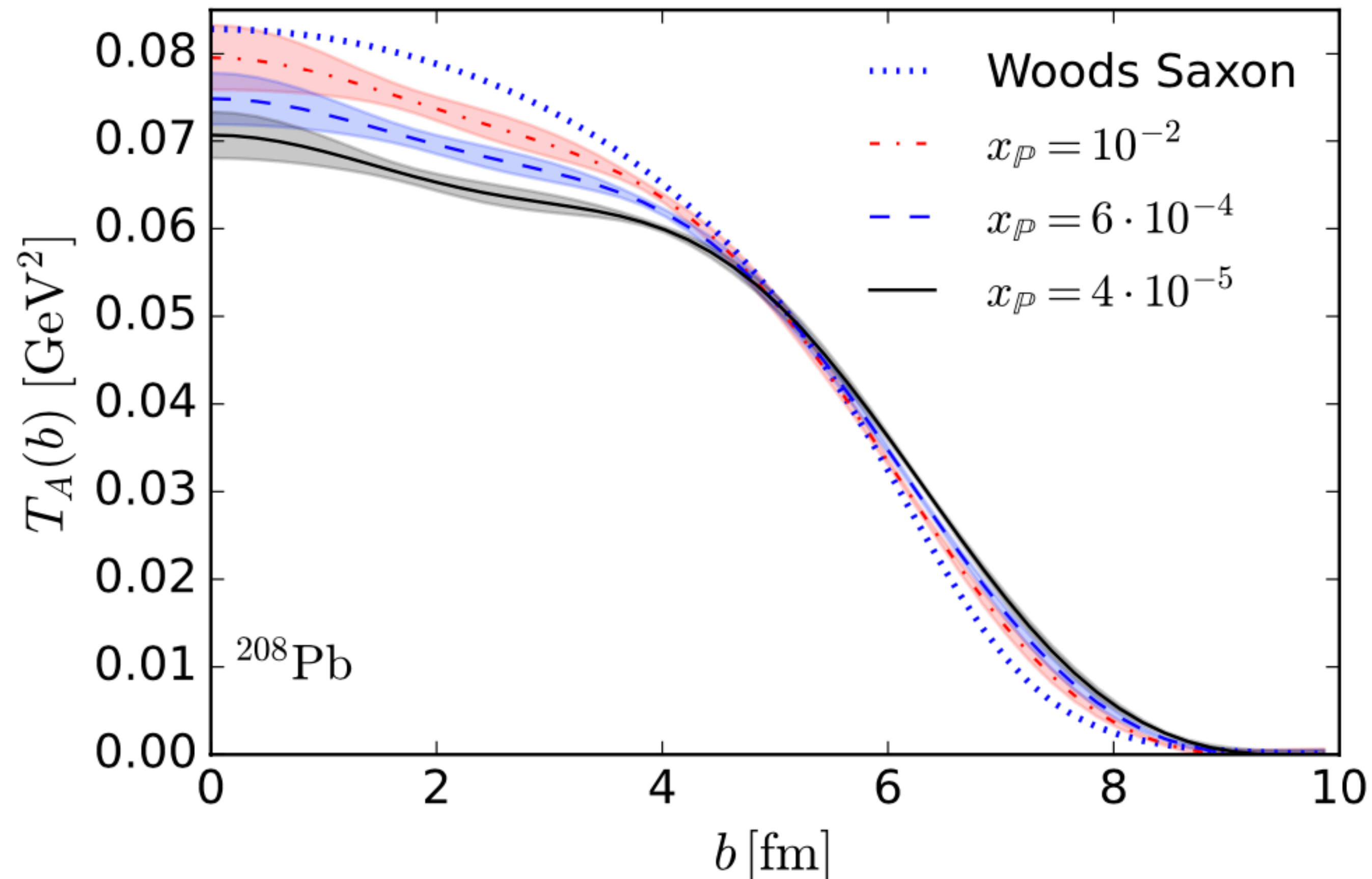
ALICE Collaboration, *Phys.Lett.B* 817 (2021) 136280

Saturation effects improve agreement with experimental data significantly

Saturation effects on nuclear geometry

H. Mäntysaari, F. Salazar, B. Schenke, Phys.Rev.D 106 (2022) 7, 074019

Fourier transform to coordinate space



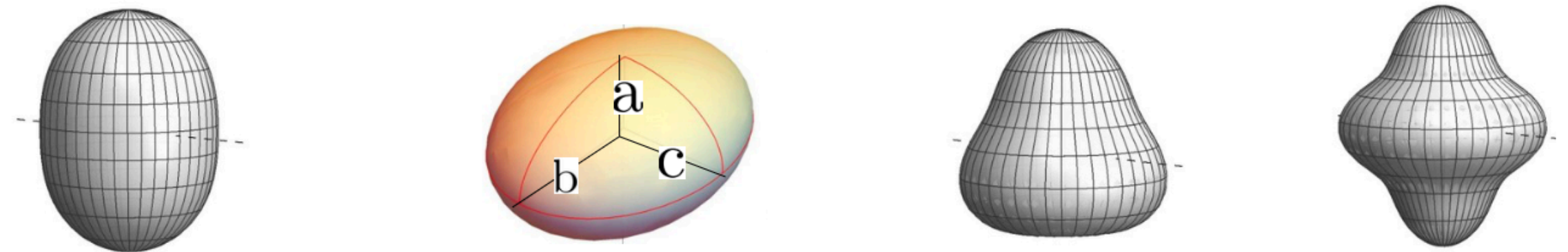
JIMWLK evolution leads to growth of the nucleus towards small x and depletion near the center (normalized so $\int d^2b T_A(b) = 208$)

Effects of deformation on diffractive cross sections

H. Mäntysaari, B. Schenke, C. Shen, W. Zhao, arXiv:2303.04866

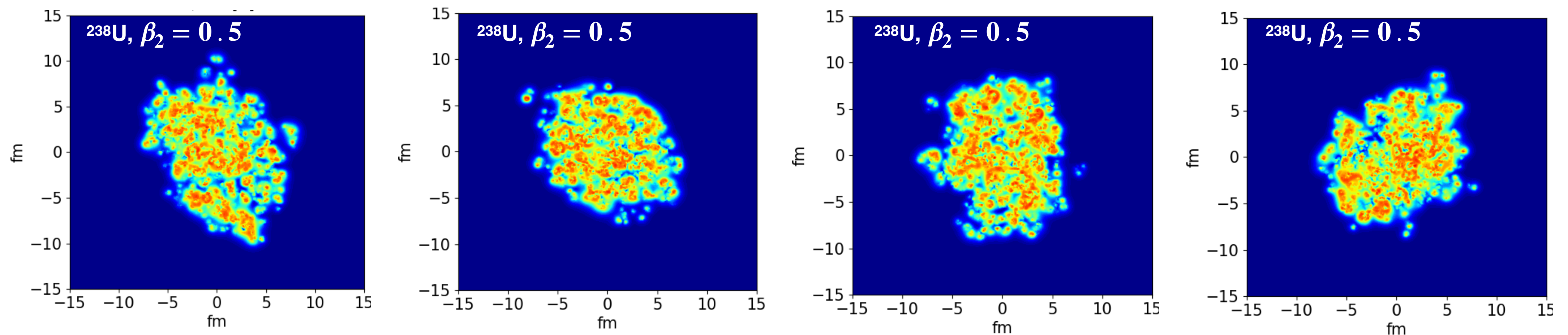
Implement deformation in the Woods-Saxon distribution:

$$\rho(r, \Theta, \Phi) \propto \frac{1}{1 + \exp([r - R(\Theta, \Phi)]/a)}, \quad R(\Theta, \Phi) = R_0 \left[1 + \beta_2 \left(\cos \gamma Y_{20}(\Theta) + \sin \gamma Y_{22}(\Theta, \Phi) \right) + \beta_3 Y_{30}(\Theta) + \beta_4 Y_{40}(\Theta) \right]$$



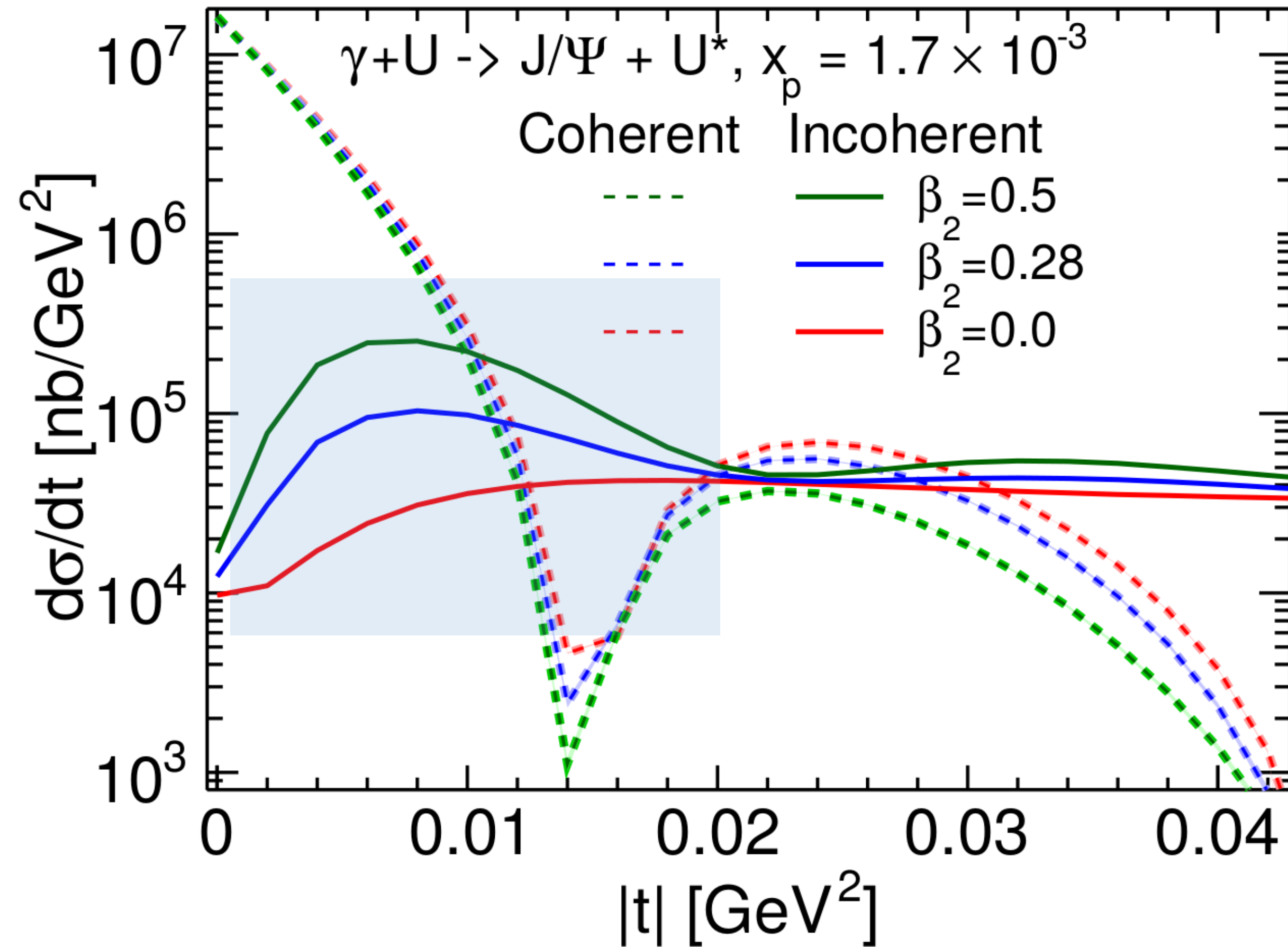
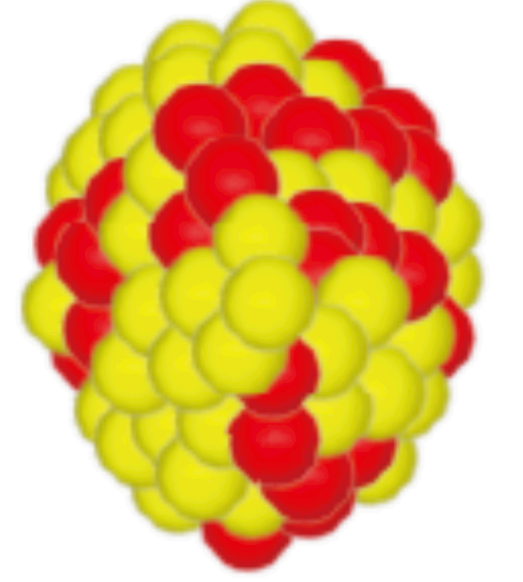
from G. Giacalone

Deformed nuclei exhibit larger fluctuation in the transverse projection:



Effects of deformation on diffractive cross sections: Uranium

H. Mäntysaari, B. Schenke, C. Shen, W. Zhao, arXiv:2303.04866



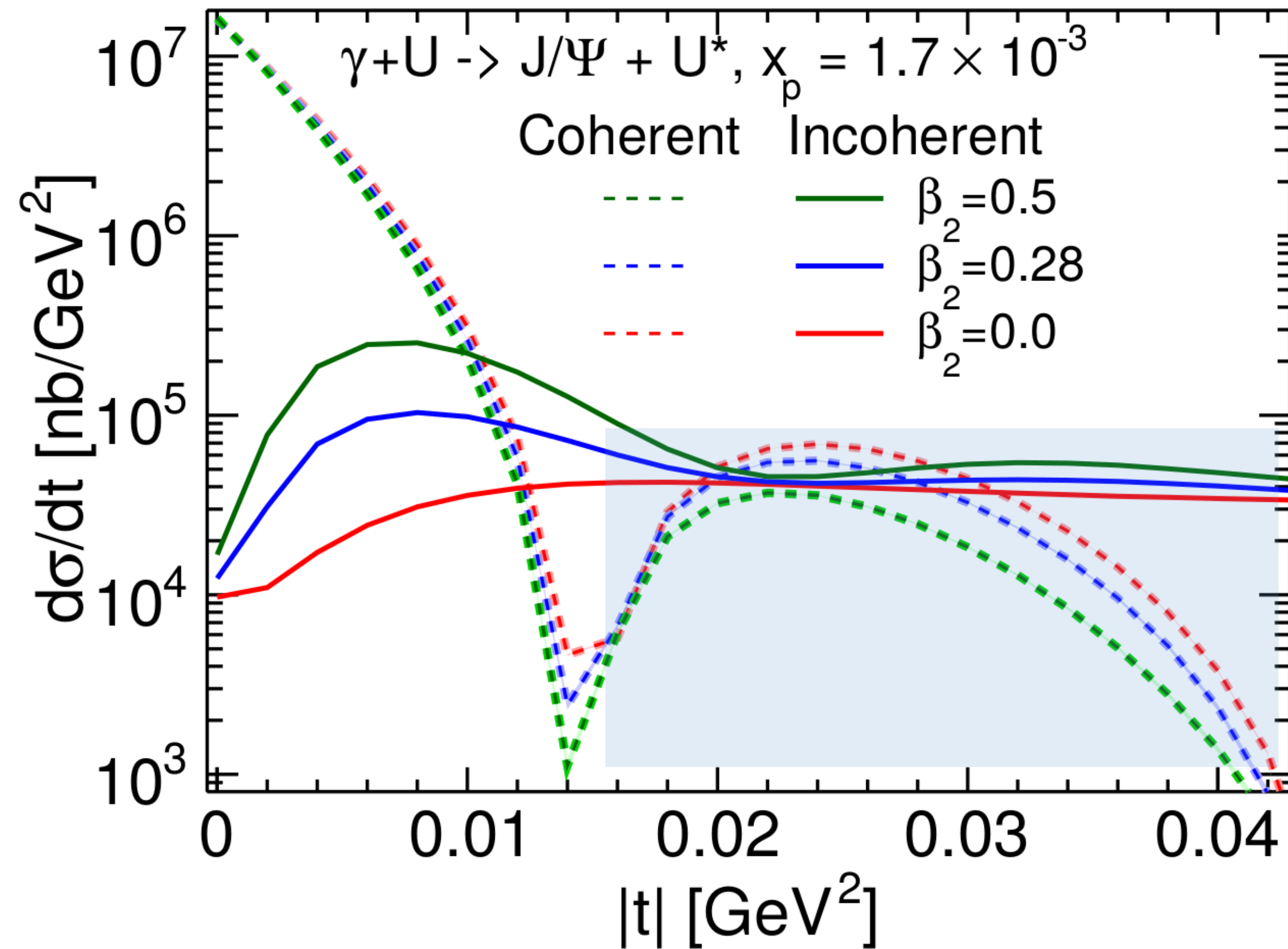
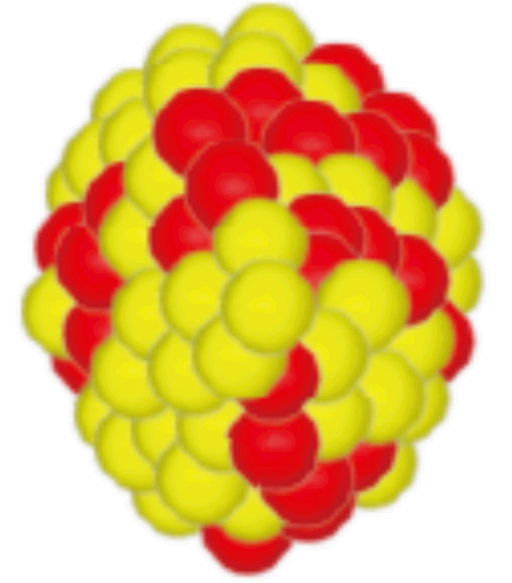
Deformation of the nucleus affects incoherent cross section at small $|t|$ (large length scales)

This observable provides direct information on the small x structure

$$Q^2 = 0$$

Effects of deformation on diffractive cross sections: Uranium

H. Mäntysaari, B. Schenke, C. Shen, W. Zhao, arXiv:2303.04866



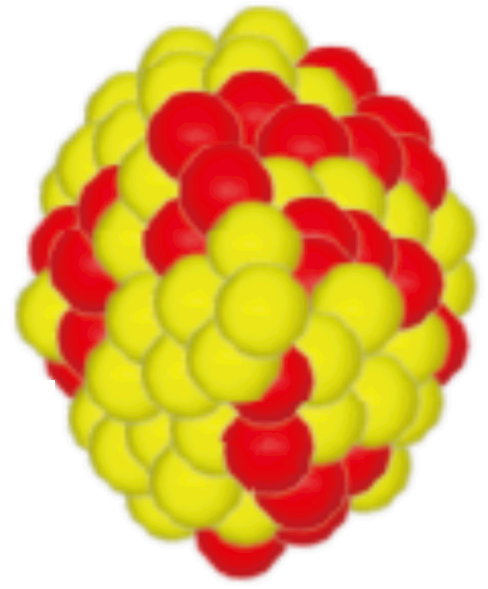
Deformation changes the shape of the average 2D projection of the nucleus



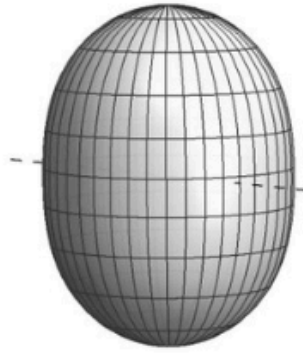
Modification of the coherent cross section

Effects of deformation on diffractive cross sections: Uranium

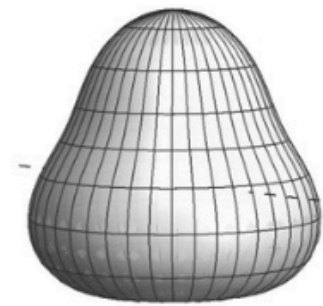
H. Mäntysaari, B. Schenke, C. Shen, W. Zhao, arXiv:2303.04866



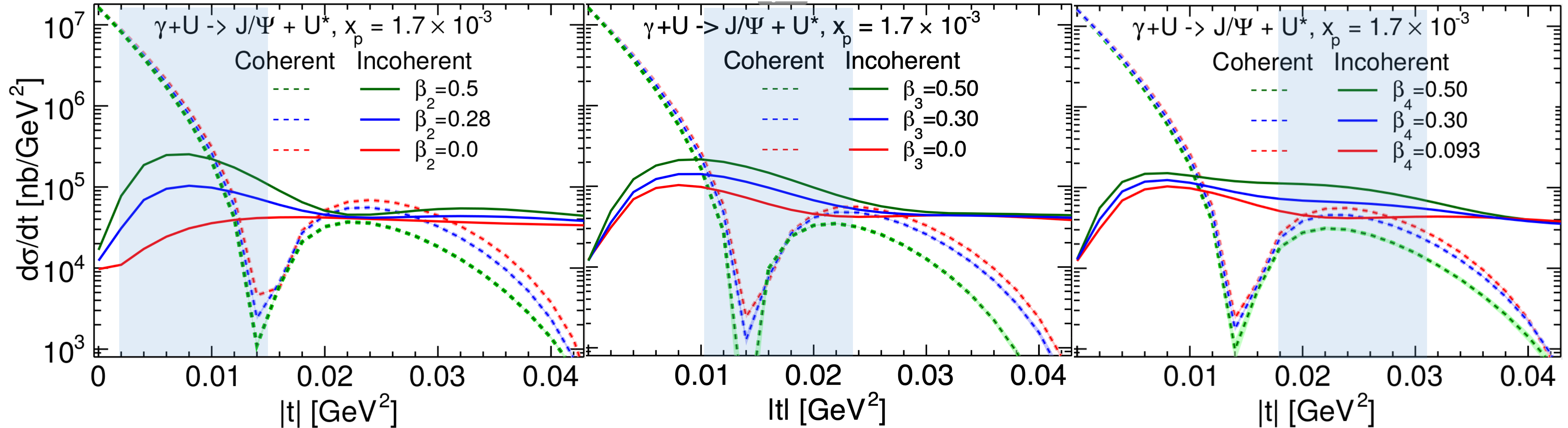
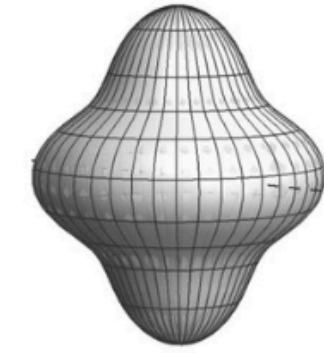
β_2



β_3



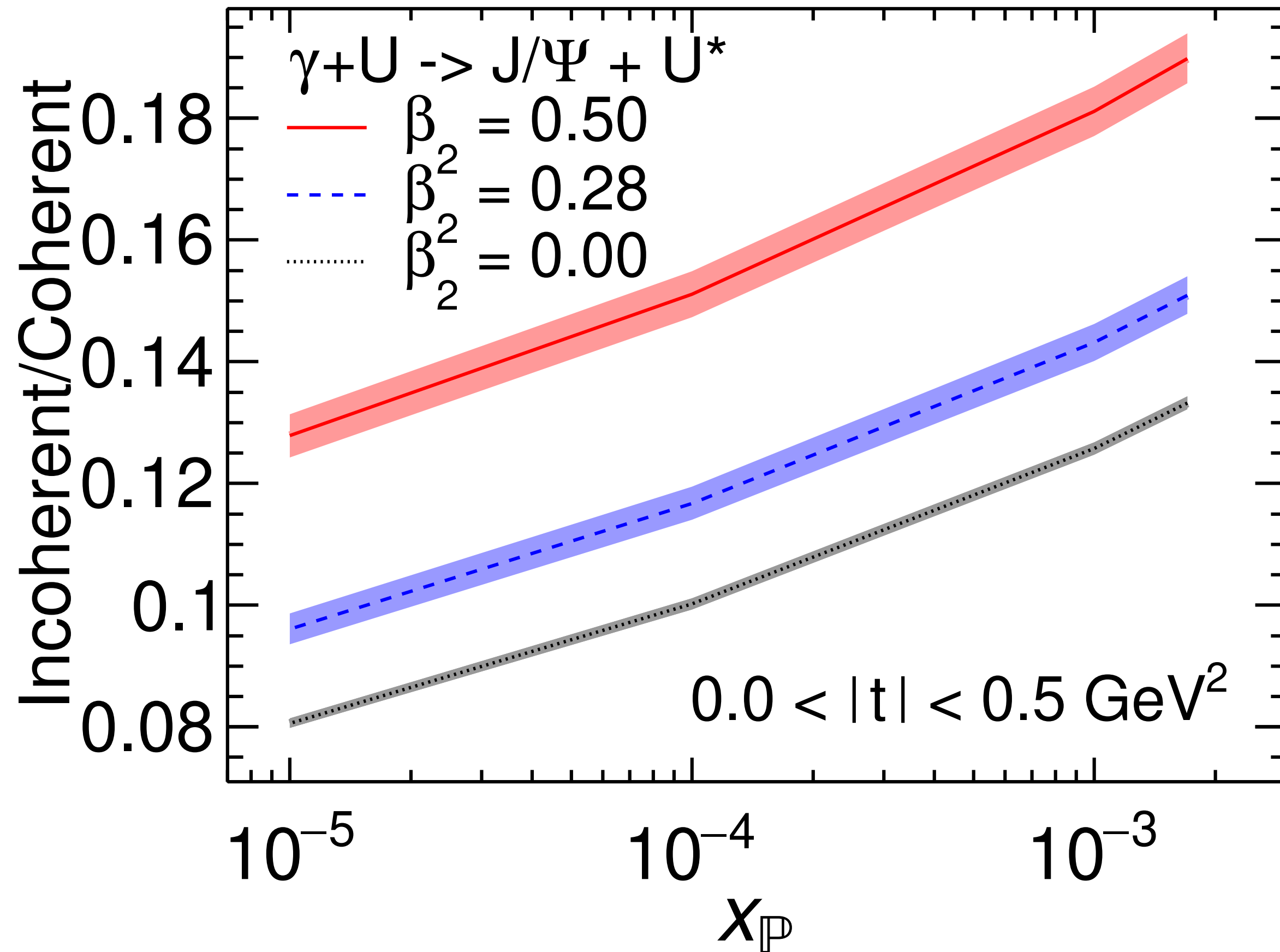
β_4



- β_2 , β_3 and β_4 modify fluctuations at different length scales:
Change incoherent cross section in different $|t|$ regions

Towards smaller x

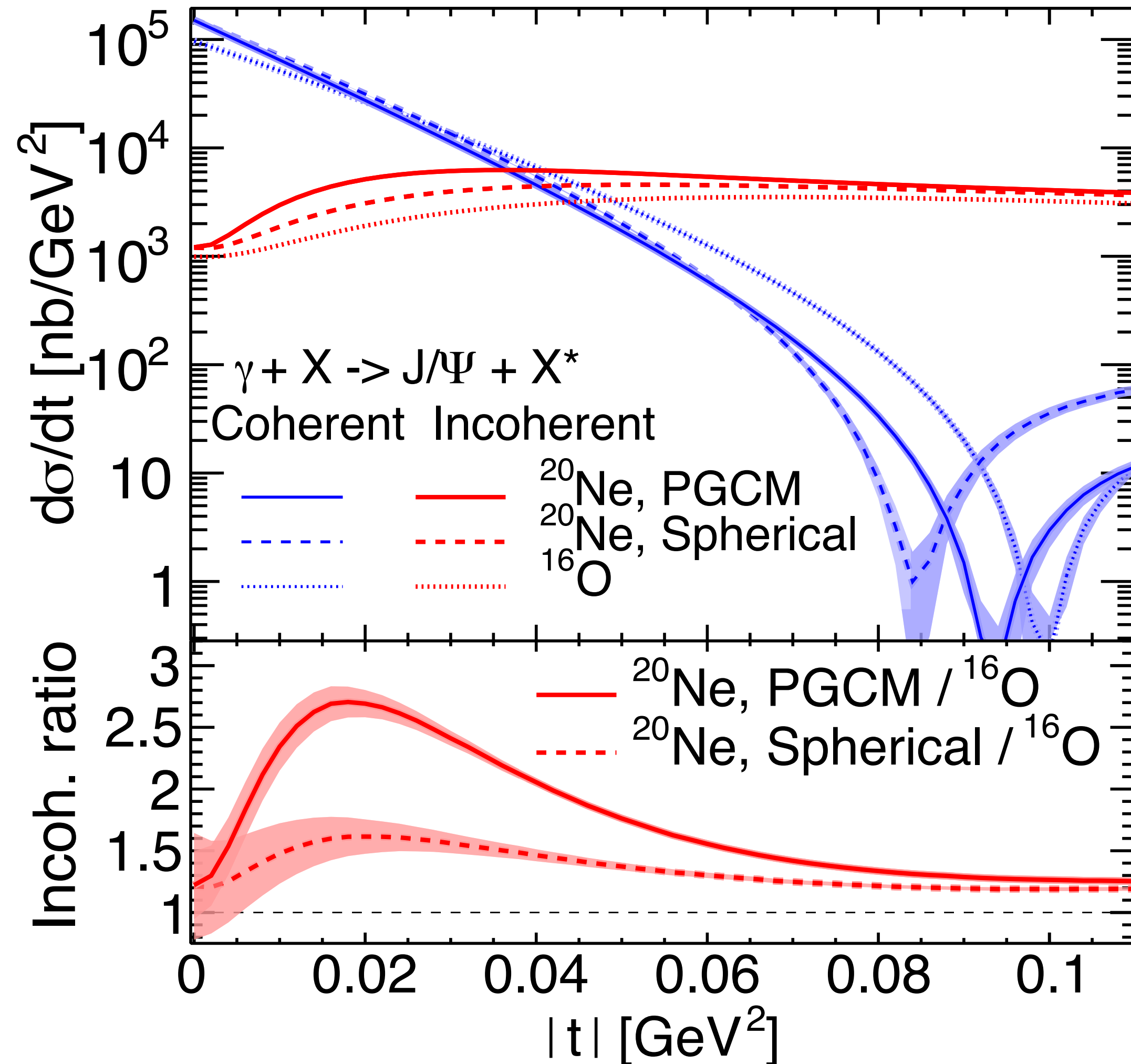
H. Mäntysaari, B. Schenke, C. Shen, W. Zhao, arXiv:2303.04866



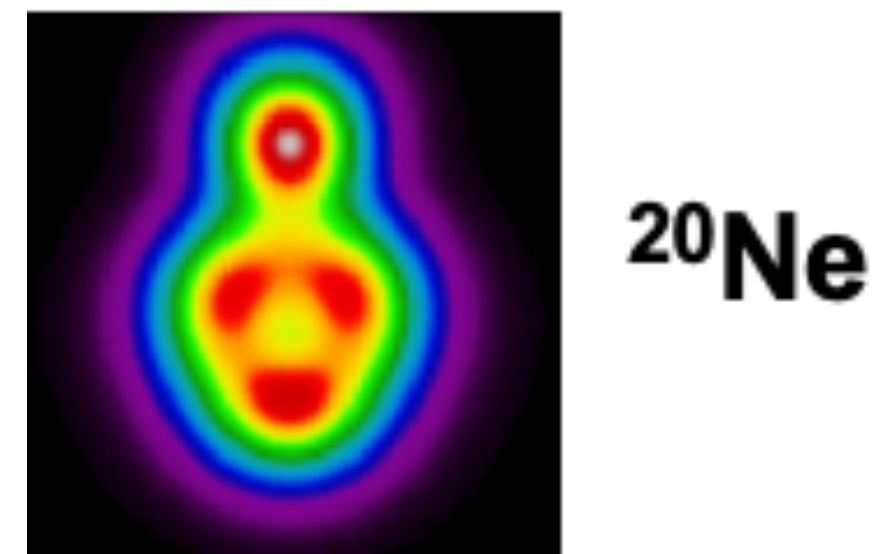
- JIMWLK evolution to smaller x
- Both cross sections increase
- Ratio incoherent/coherent decreases because fluctuations are reduced (nucleus becomes smoother)
- Difference between different β_2 does not decrease noticeably in this x range
- Is there a large enough x range we can cover at the EIC (at least $10^{-3} - 10^{-2}$)?

Neon and Oxygen targets

H. Mäntysaari, B. Schenke, C. Shen, W. Zhao, arXiv:2303.04866



- ²⁰Ne has a bowling pin shape that leads to an increased incoherent cross section relative to an assumed spherical (on average) neon or a spherical oxygen

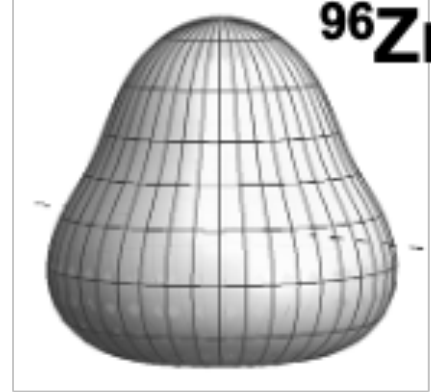


PGCM: Projected Generator Coordinate Method: B. Bally et al., “Deciphering small system collectivity with bowling-pin-shaped ²⁰Ne isotopes,” in preparation (2023); Mikael Frosini, Thomas Duguet, Jean-Paul Ebran, Benjamin Bally, Tobias Mongelli, Tomá’s R. Rodríguez, Robert Roth, and Vittorio Soma, Eur. Phys. J. A 58, 63 (2022)

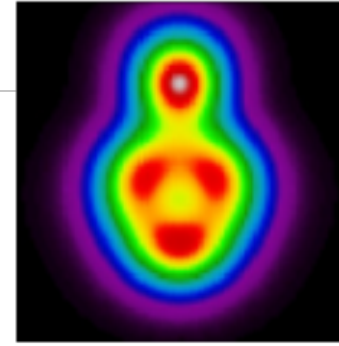
Multi-scale sensitivity

Nuclear deformations

^{238}U



^{96}Zr



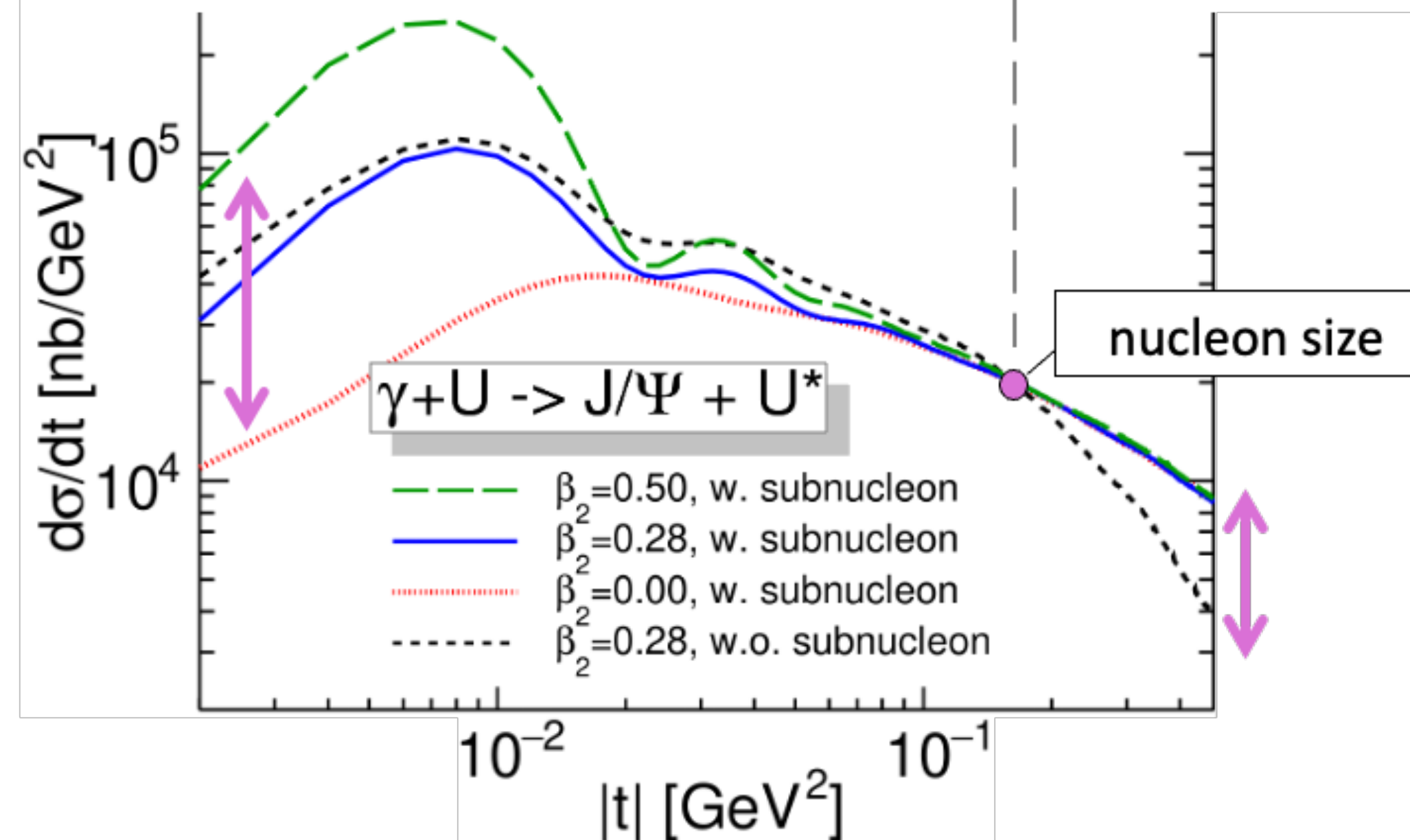
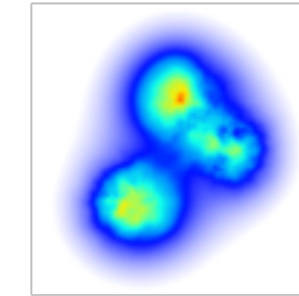
^{20}Ne

Short-range correlations

10 fm

1 fm

0.1 fm



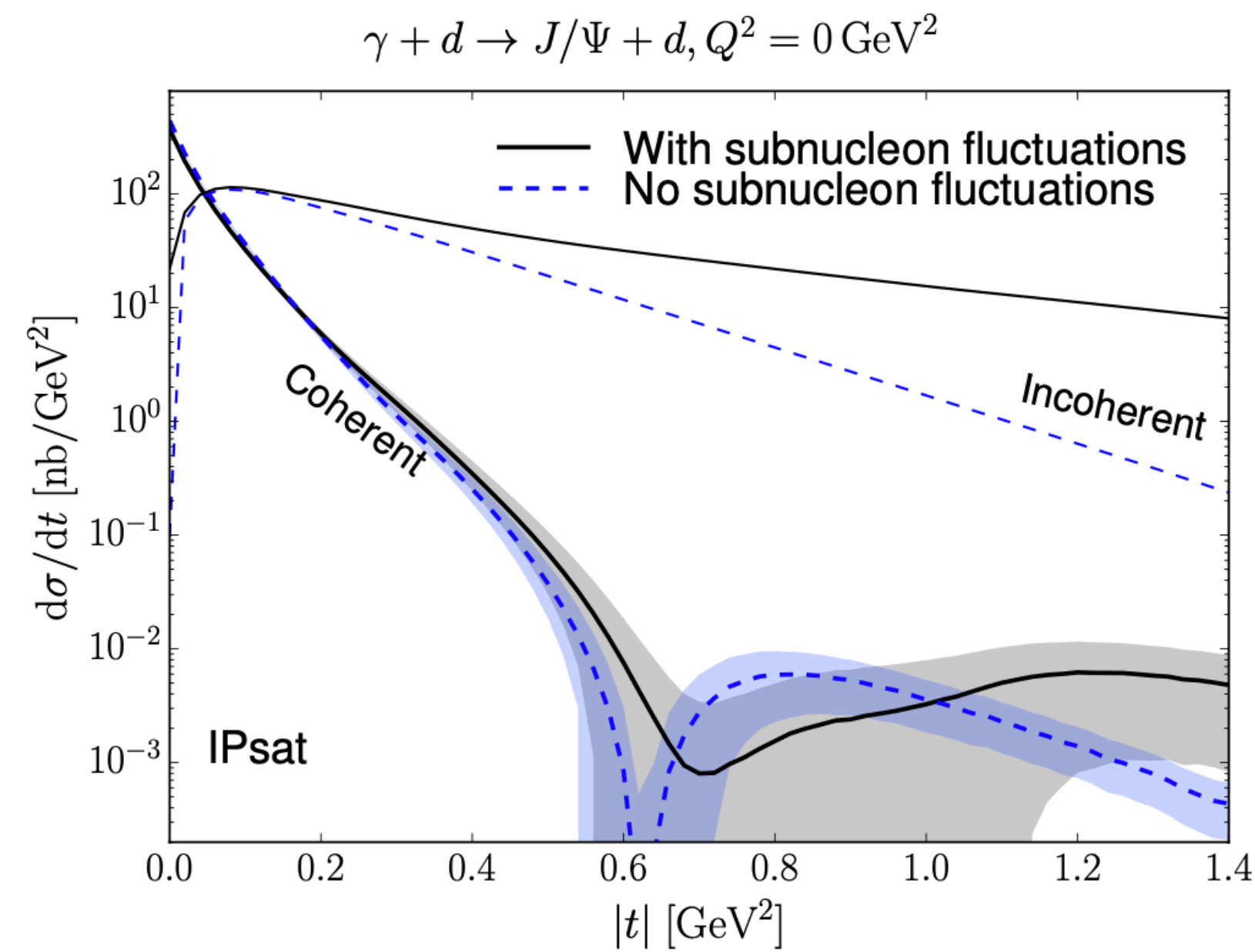
Chiral effective field theory
(low-energy QCD)



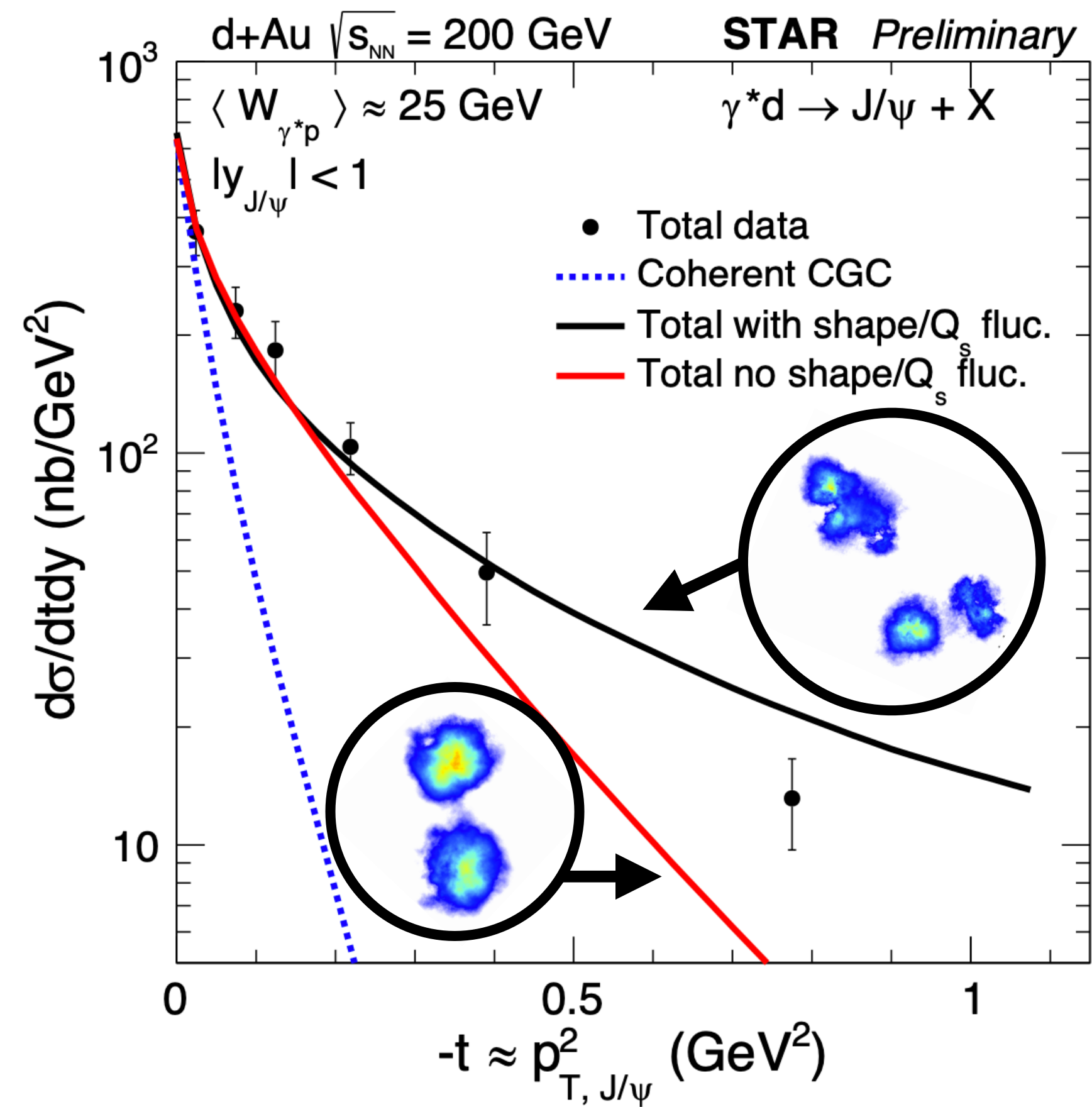
CGC effective field theory
(high-energy QCD)

Photoproduction of J/ψ in d+Au collisions at STAR

H. Mäntysaari, B. Schenke, Phys. Rev. C101, 015203 (2020)



Can also access details of deuteron wave function (BACKUP)



Substructure: large effect on incoherent at $|t| \gtrsim 0.25 \text{ GeV}^2$ (as in Pb)

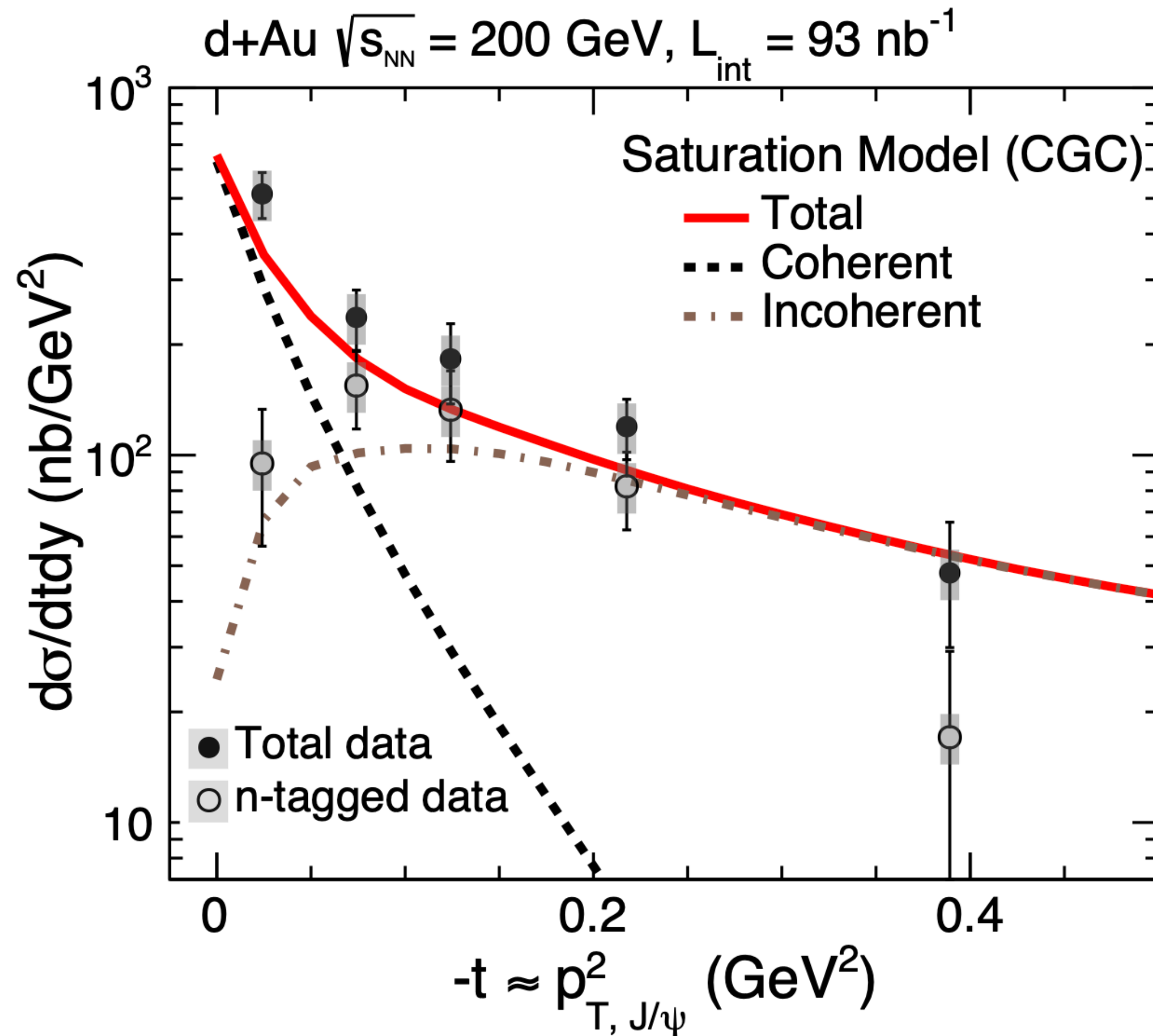
STAR data favors substructure

STAR Collaboration at Hard Probes 2020

PoS HardProbes2020 (2021) 100; arXiv:2009.04860

Photoproduction of J/ψ in d+Au collisions at STAR

H. Mäntysaari, B. Schenke, Phys. Rev. C101, 015203 (2020)



n-tagged results can be compared to incoherent cross section

STAR Collaboration, Phys. Rev. Lett. 128, 122303, (2022) e-Print: 2109.07625

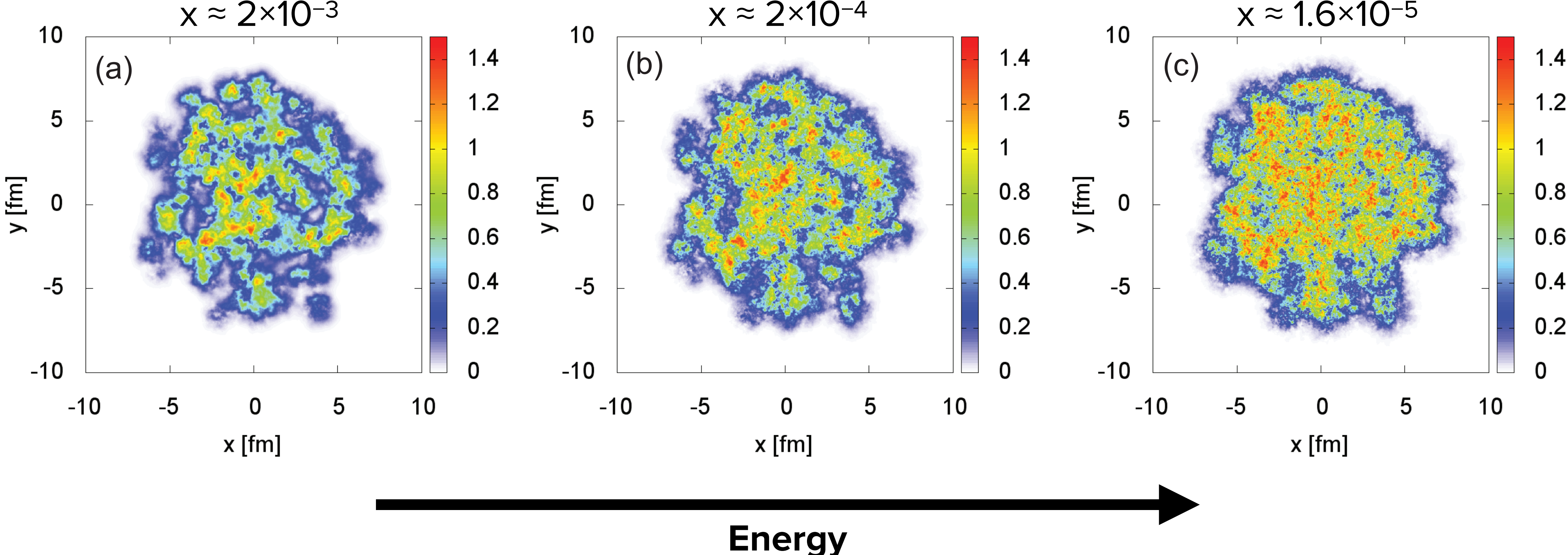
SUMMARY

- $|t|$ -differential incoherent cross section is sensitive to fluctuations at different length scales: Effects of deformation, nucleon-, and sub-nucleon fluctuations
- This means:
 1. Precision comparison of models to data requires taking deformation into account
 2. Access to nuclear structure over 2 orders of magnitude in length scales!
- What we need:
 - Separate incoherent from coherent in forward direction
 - Detect leptons from mid rapidity to backward rapidity (cover some x -range); or study other vector mesons (like ρ and detect pions)

BACKUP

JIMWLK evolution

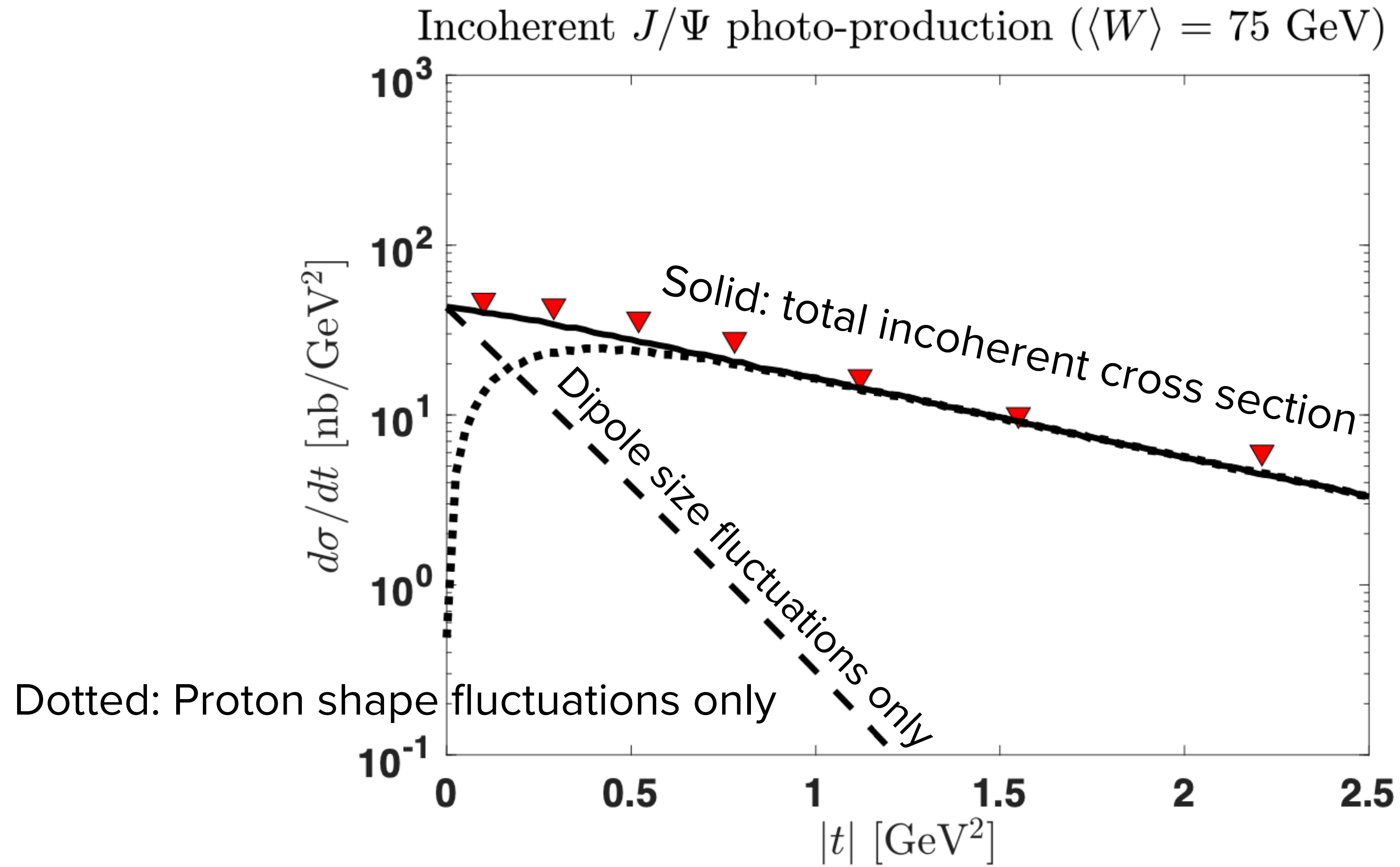
How does energy evolution affect the nuclear structure?



B. Schenke, S. Schlichting, Phys.Rev.C 94 (2016) 4, 044907

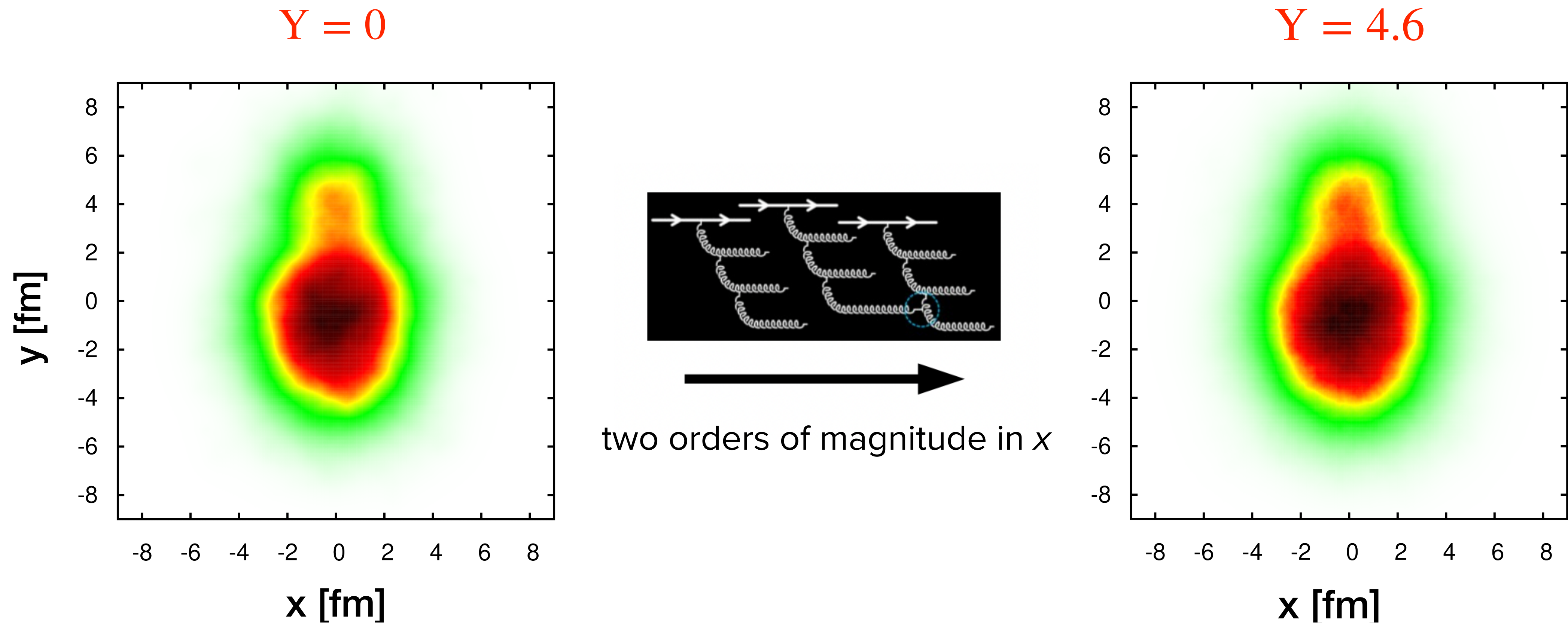
Dipole size fluctuations

Blaizot and Traini, 2209.15545 [hep-ph]



Neon - JIMWLK evolution

G. Giacalone, B. Schenke, S. Schlichting, P. Singh, in progress

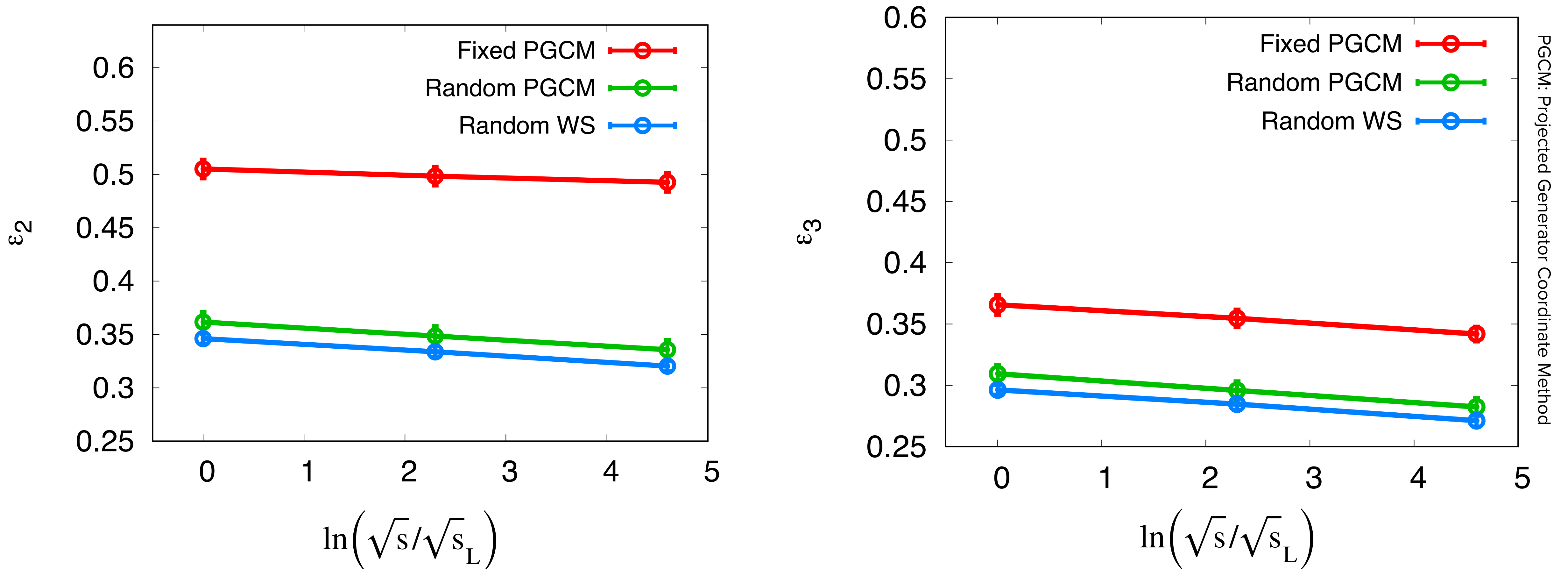


- Small- x evolution does not melt the bowling pin shape

Neon+Neon collisions - JIMWLK evolution

G. Giacalone, B. Schenke, S. Schlichting, P. Singh, in progress

- After the collision at different energies (x), measure the spatial eccentricities



- Expected reduction - smoother distributions, but no large change

Light nuclei: Nucleon distributions

H. Mäntysaari, B. Schenke, *Phys. Rev. C*101, 015203 (2020)

Nucleon distributions:

- Deuteron wave function:

- Argonne v18 (AV18)

R. B. Wiringa, V. G. J. Stoks and R. Schiavilla, *Phys. Rev. C*51 (1995) 38
www.phy.anl.gov/theory/research/density2

- Hulthen:

$$\phi_{pn}(d_{pn}) = \frac{1}{\sqrt{2\pi}} \frac{\sqrt{ab(a+b)} e^{-ad_{pn}} - e^{-bd_{pn}}}{b-a} \frac{1}{d_{pn}} \quad \begin{aligned} a &= 0.228\text{fm}^{-1} \\ b &= 1.18\text{fm}^{-1} \end{aligned}$$

see M. L. Miller, K. Reygers, S. J. Sanders, P. Steinberg, *Ann. Rev. Nucl. Part. Sci.* 57 (2007) 205

- ^3He wave function:

- AV18+UIX J. Carlson and R. Schiavilla, *Rev. Mod. Phys.* 70 (1998) 743

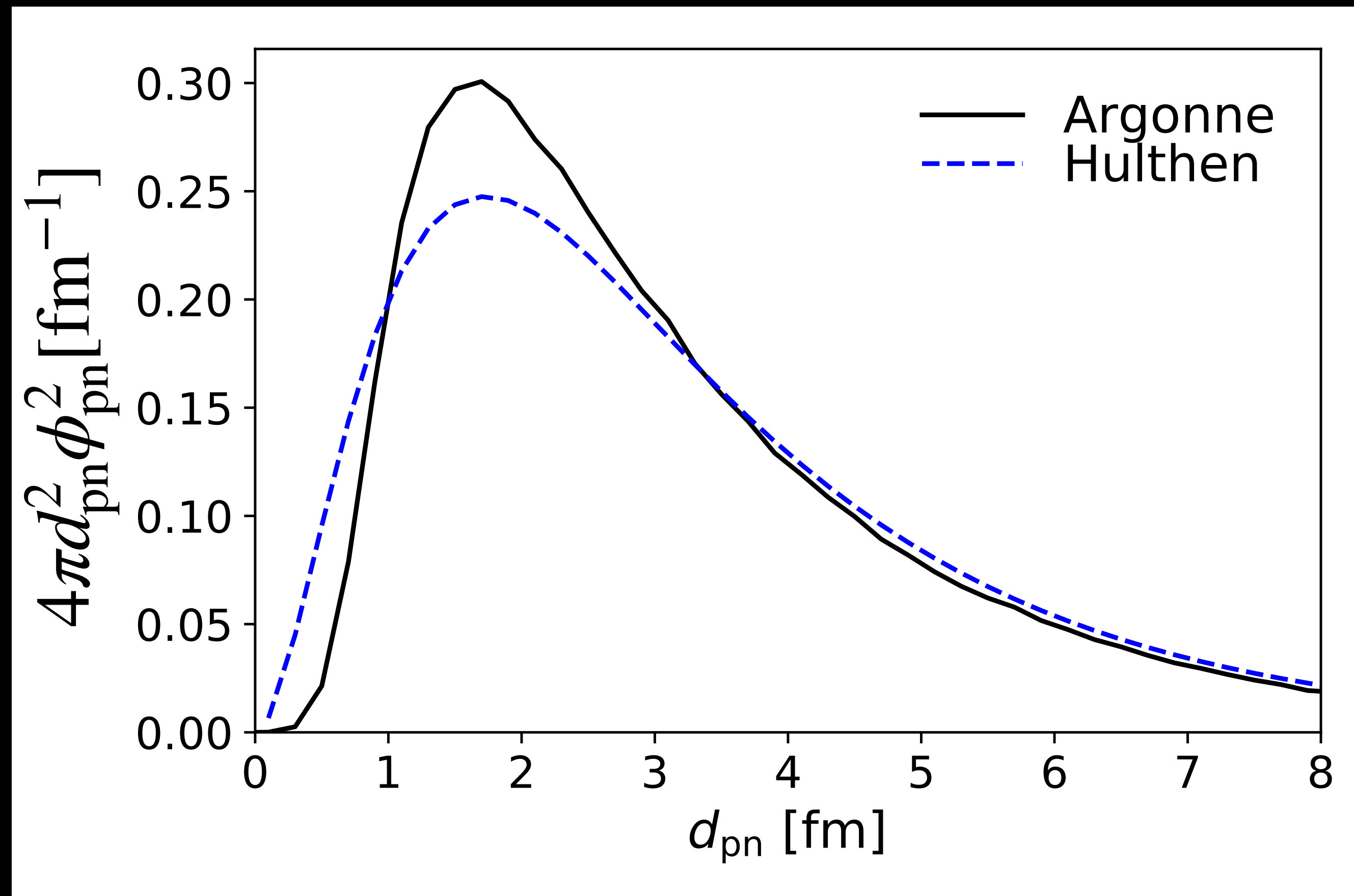
same configurations as available in PHOBOS MC-Glauber

C. Loizides, J. Nagle and P. Steinberg, [arXiv:1408.2549](https://arxiv.org/abs/1408.2549)

Light nuclei: Nucleon distributions

H. Mäntysaari, B. Schenke, *Phys. Rev. C*101, 015203 (2020)

Deuteron size distributions



We need the gluon distribution

Assumption:

Small x gluon structure follows the large x nucleon structure

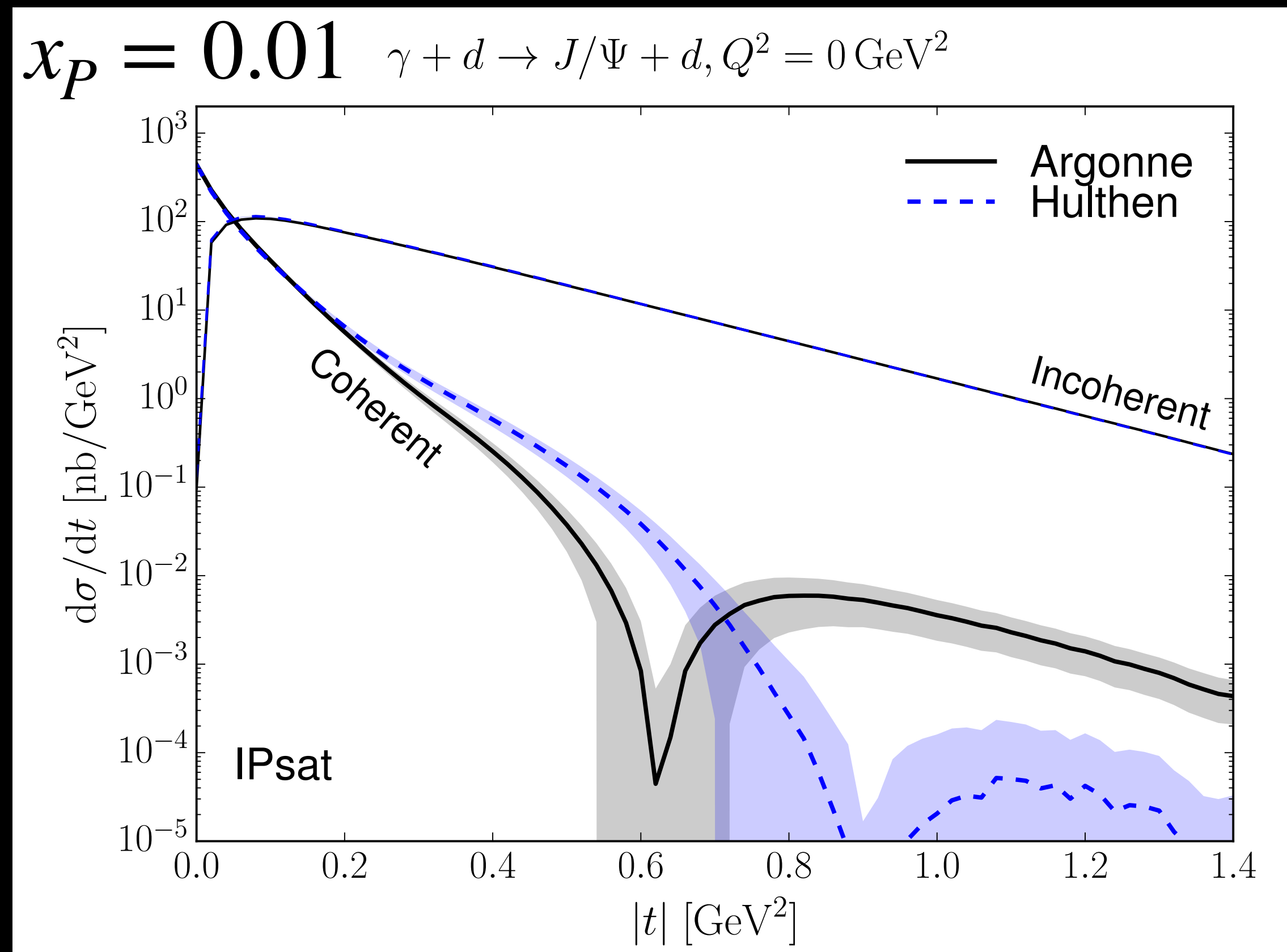
Predictions for the EIC: Effect of deuteron wave function

H. Mäntysaari, B. Schenke, *Phys. Rev. C*101, 015203 (2020)

J/Ψ production for $\sqrt{s} = 140\sqrt{Z/A}$ GeV

such that x_p can reach down to 10^{-4} to 10^{-3}

$$x_p = \frac{Q^2 + M_V^2 - t}{Q^2 + W^2 - m_N^2}$$



Differences appear at $|t| \gtrsim 0.3 \text{ GeV}^2$
(Long distance behavior is similar)

The two wave functions result in similar rms sizes of the deuteron

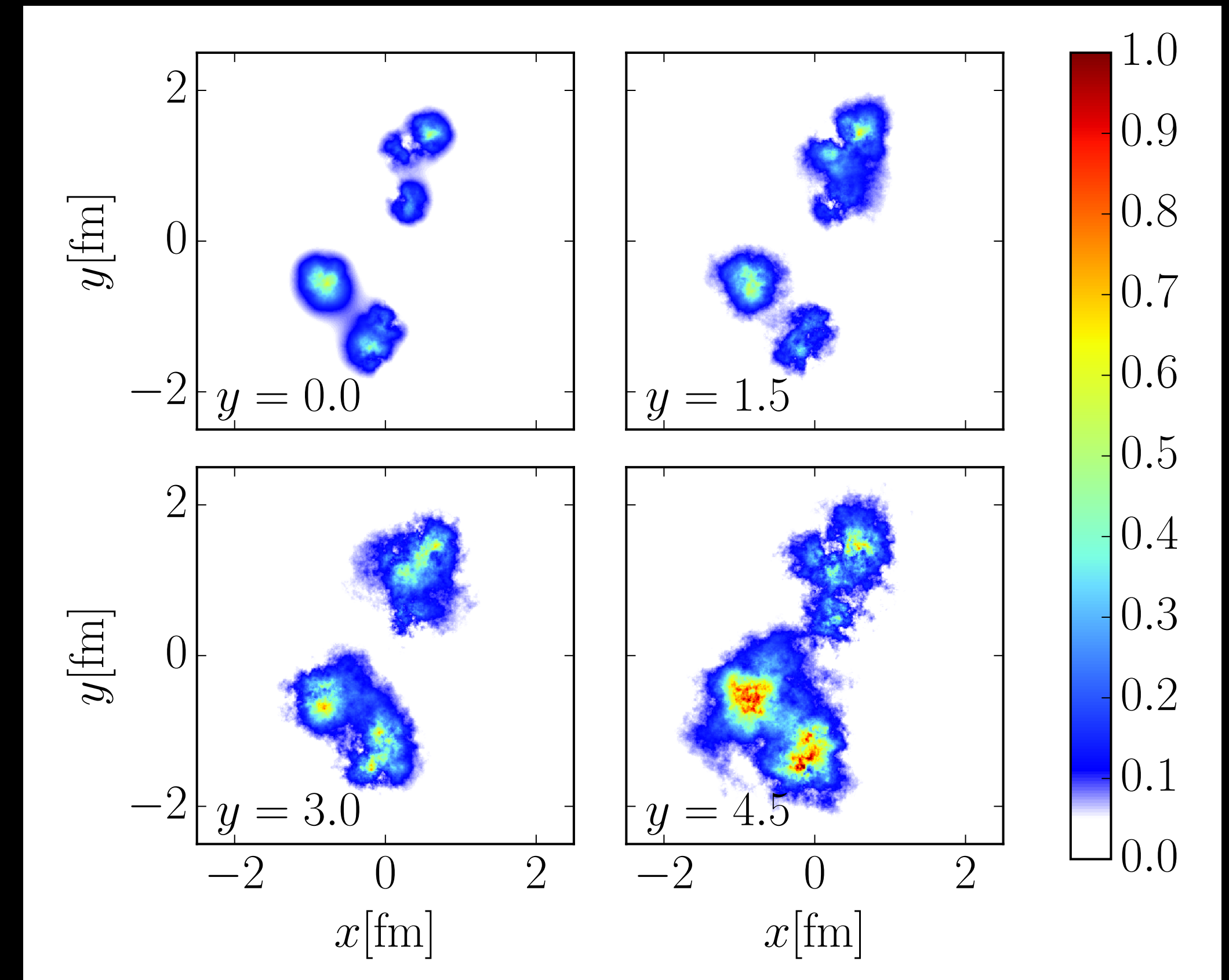
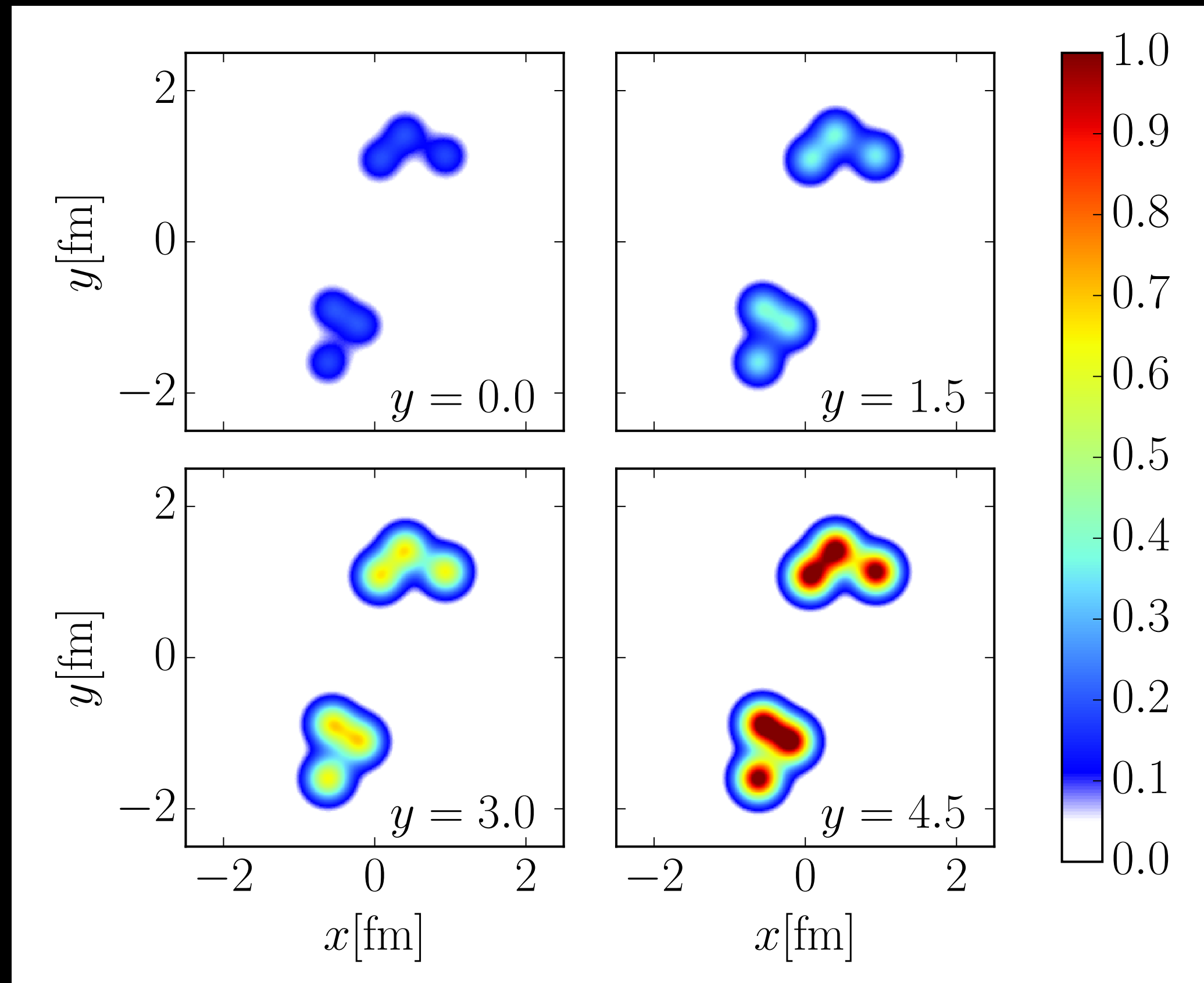
Difference in dip position must come from the different average impact parameter profile.

Energy evolution (deuterons)

H. Mäntysaari, B. Schenke, Phys. Rev. C101, 015203 (2020)

IPSat - only normalization changes

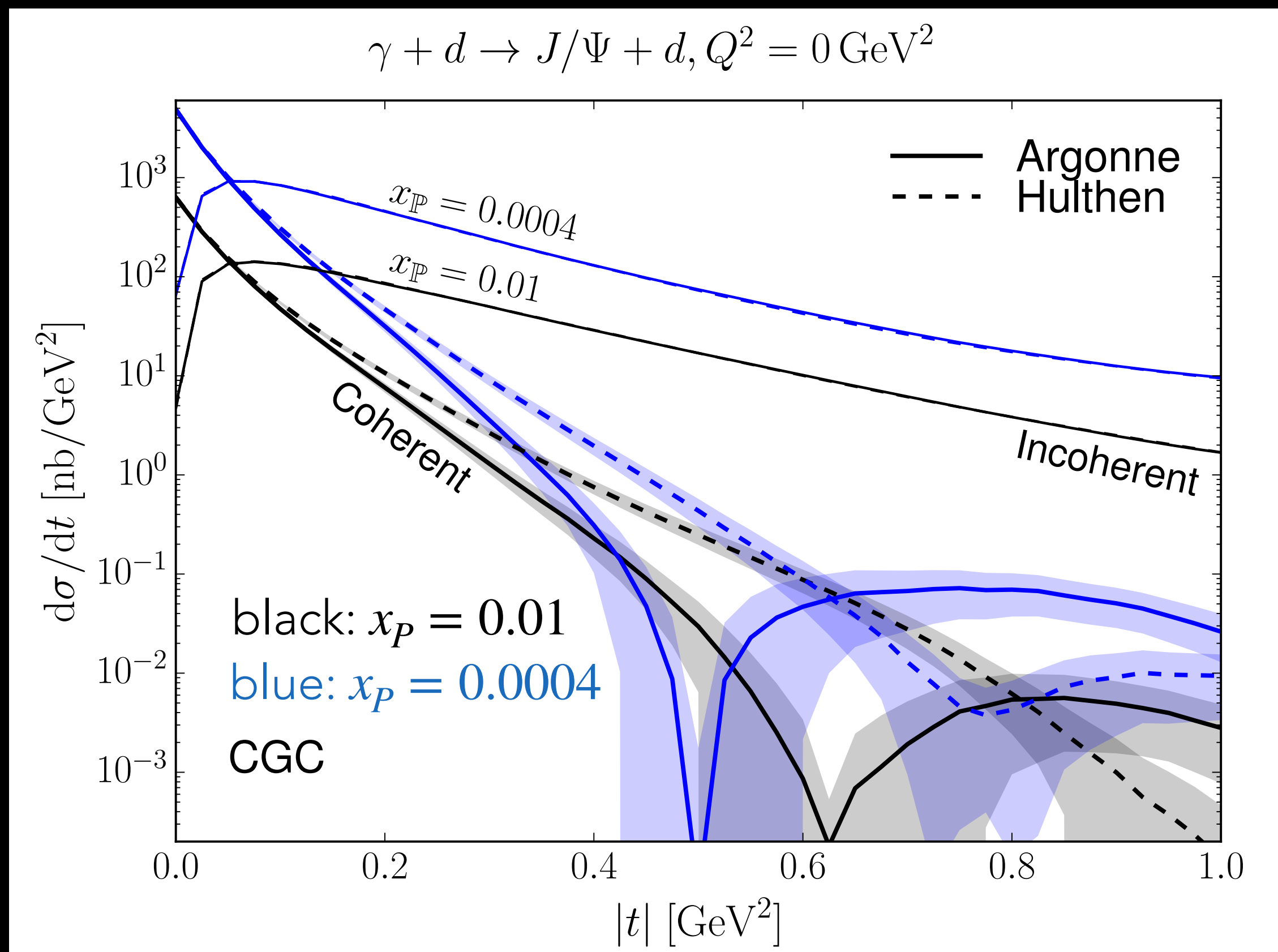
CGC - nucleus grows as well



We plot $1 - \text{Re}[\text{tr}(V(\vec{x}))]/N_c$

Predictions for the EIC: Small- x evolution

H. Mäntysaari, B. Schenke, *Phys. Rev. C*101, 015203 (2020)



(no nucleon shape fluctuations)

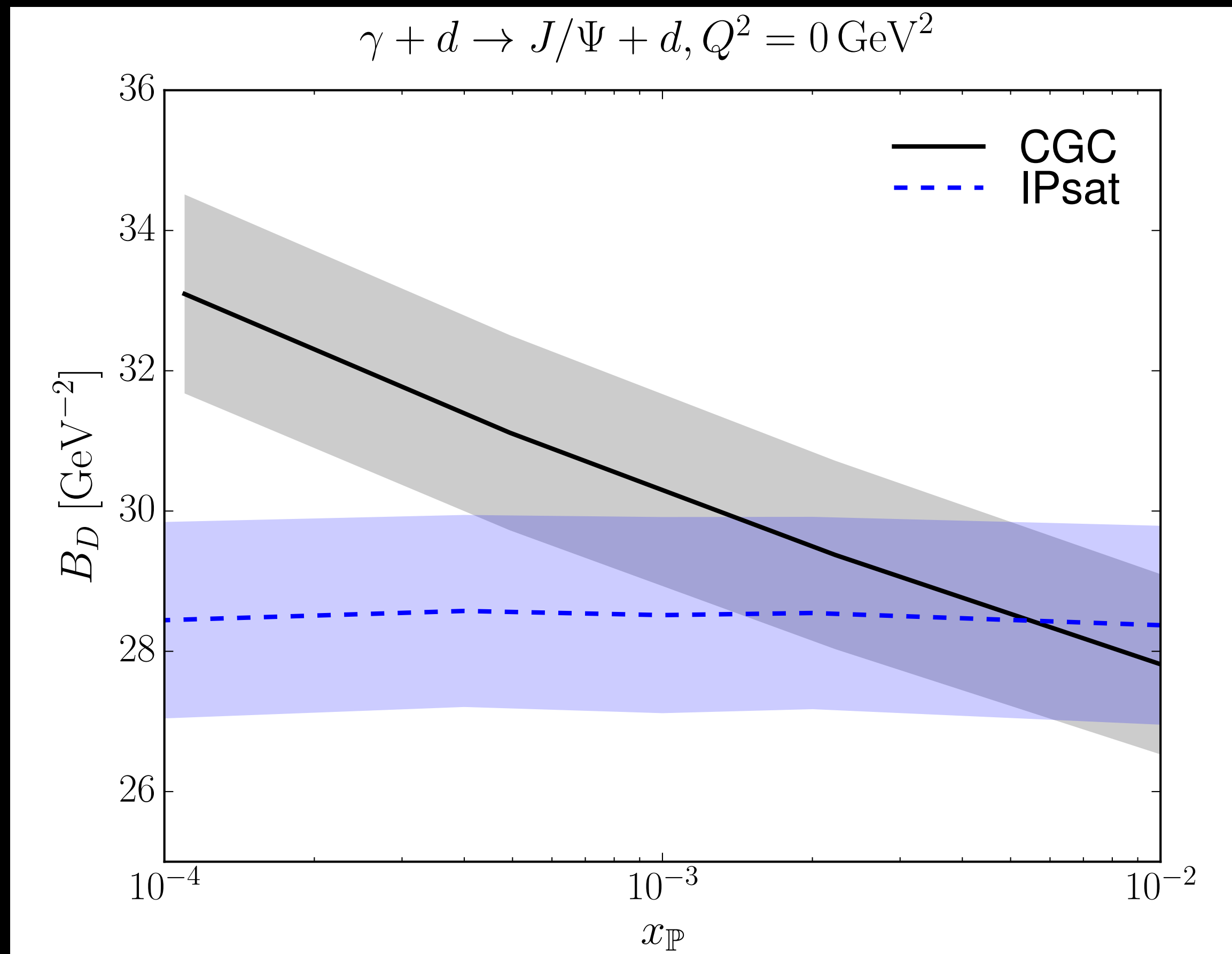
Differences between wave functions survive the JIMWLK evolution

They are not washed out at small x

Dip moves to smaller $|t|$ indicating growth of the average target size

Predictions for the EIC: Target size vs. x

H. Mäntysaari, B. Schenke, *Phys. Rev. C*101, 015203 (2020)



Growth of the target with decreasing x is illustrated by extracting B_D from a fit to the coherent cross section at small t using $d\sigma/dt \sim \exp(-B_D |t|)$

IPSat model does not include the growth of the target

Dipole amplitude in e+A scattering

H. Mäntysaari, B. Schenke, *Phys. Rev. C*101, 015203 (2020)

$$N^A(\vec{r}, \vec{b}, x) = 1 - \prod_{i=1}^A [1 - N^p(\vec{r}, \vec{b} - \vec{b}_i, x)]$$

This is equivalent to summing up the density profiles of the nucleons

We also fluctuate the normalization of Q_s^2 in each hot spot according to

$$P(\ln(Q_s^2/\langle Q_s^2 \rangle)) = \frac{1}{\sqrt{2\pi}\sigma} \exp\left[-\frac{\ln^2(Q_s^2/\langle Q_s^2 \rangle)}{2\sigma^2}\right]$$

with $\sigma = 0.65$ for IPSat

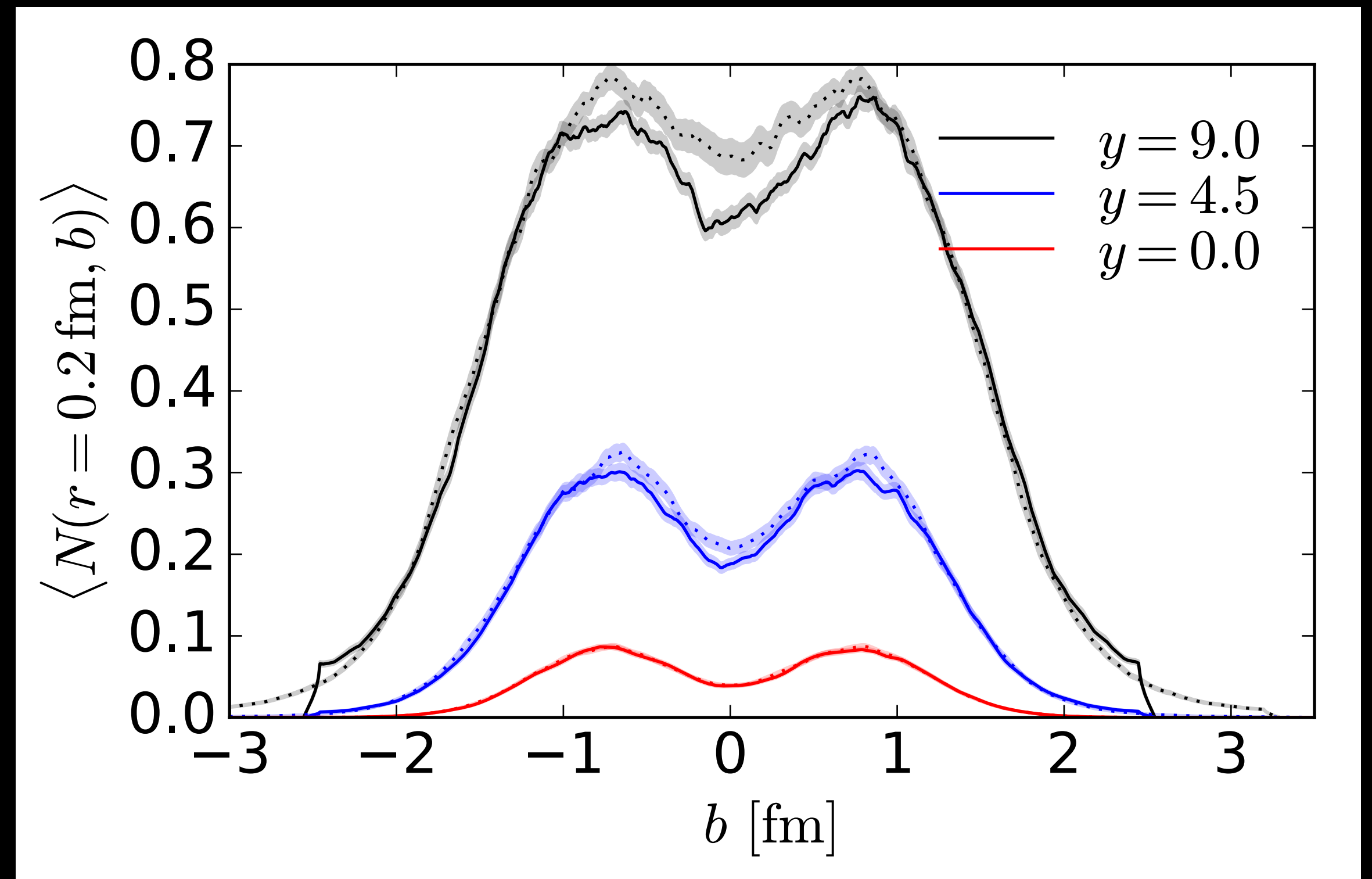
Saturation effects

H. Mäntysaari, B. Schenke, Phys. Rev. C101, 015203 (2020)

Comparing evolution of a deuteron (solid) to two individual nucleons (dotted)

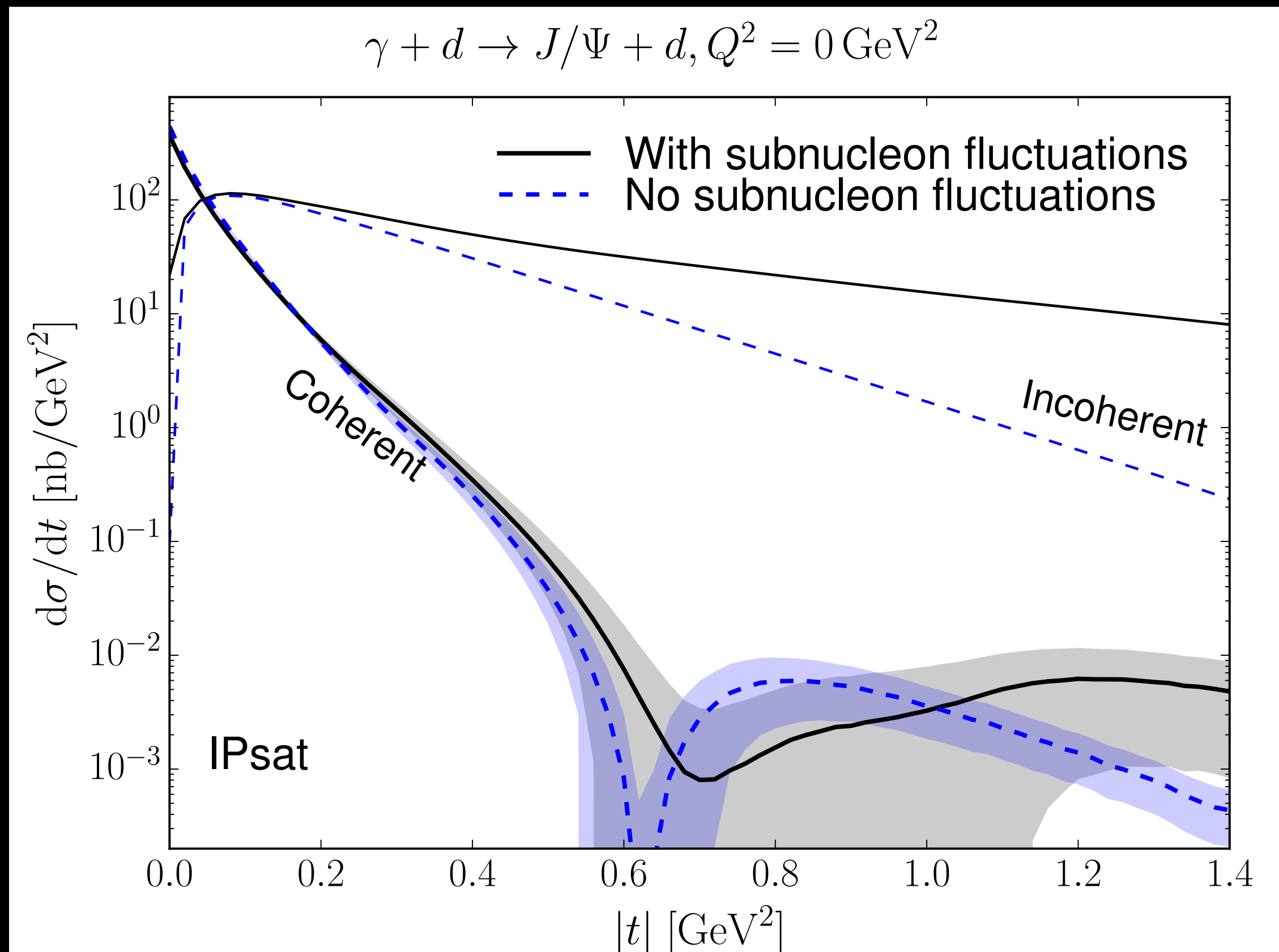
The effect is only visible after substantial evolution

$$d_{pn} = 1.5 \text{ fm}$$



Predictions for the EIC: Effect of nucleon shape fluctuations

H. Mäntysaari, B. Schenke, *Phys. Rev. C*101, 015203 (2020)



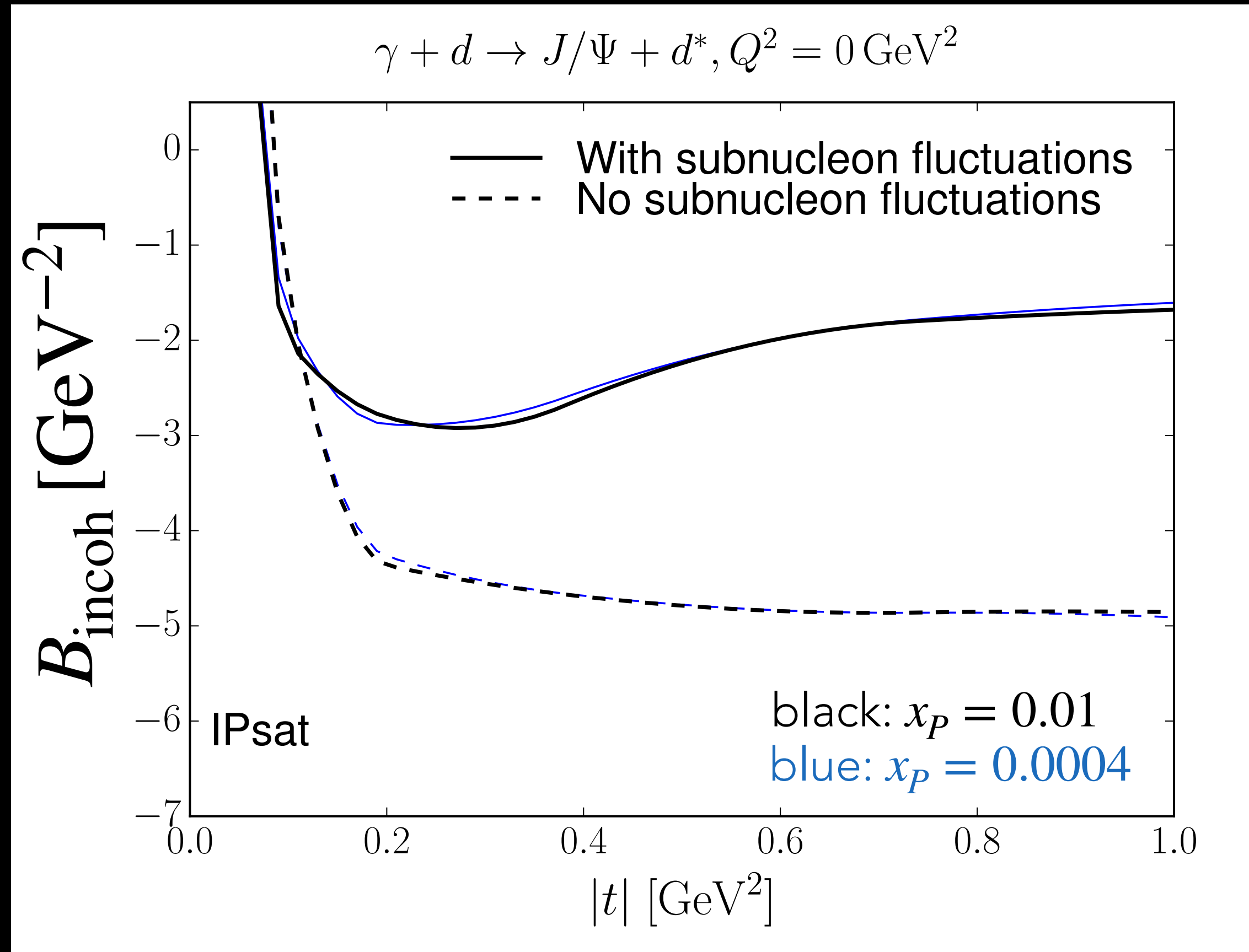
Coherent cross section unchanged (within errors) - average shape is (approximately) the same by construction

Subnucleon fluctuations increase incoherent cross section significantly for $|t| \gtrsim 0.25 \text{ GeV}^2$

Lower $|t|$ are dominated by fluctuations on larger length scales

Predictions for the EIC: Slope of incoherent cross section

H. Mäntysaari, B. Schenke, *Phys. Rev. C*101, 015203 (2020)

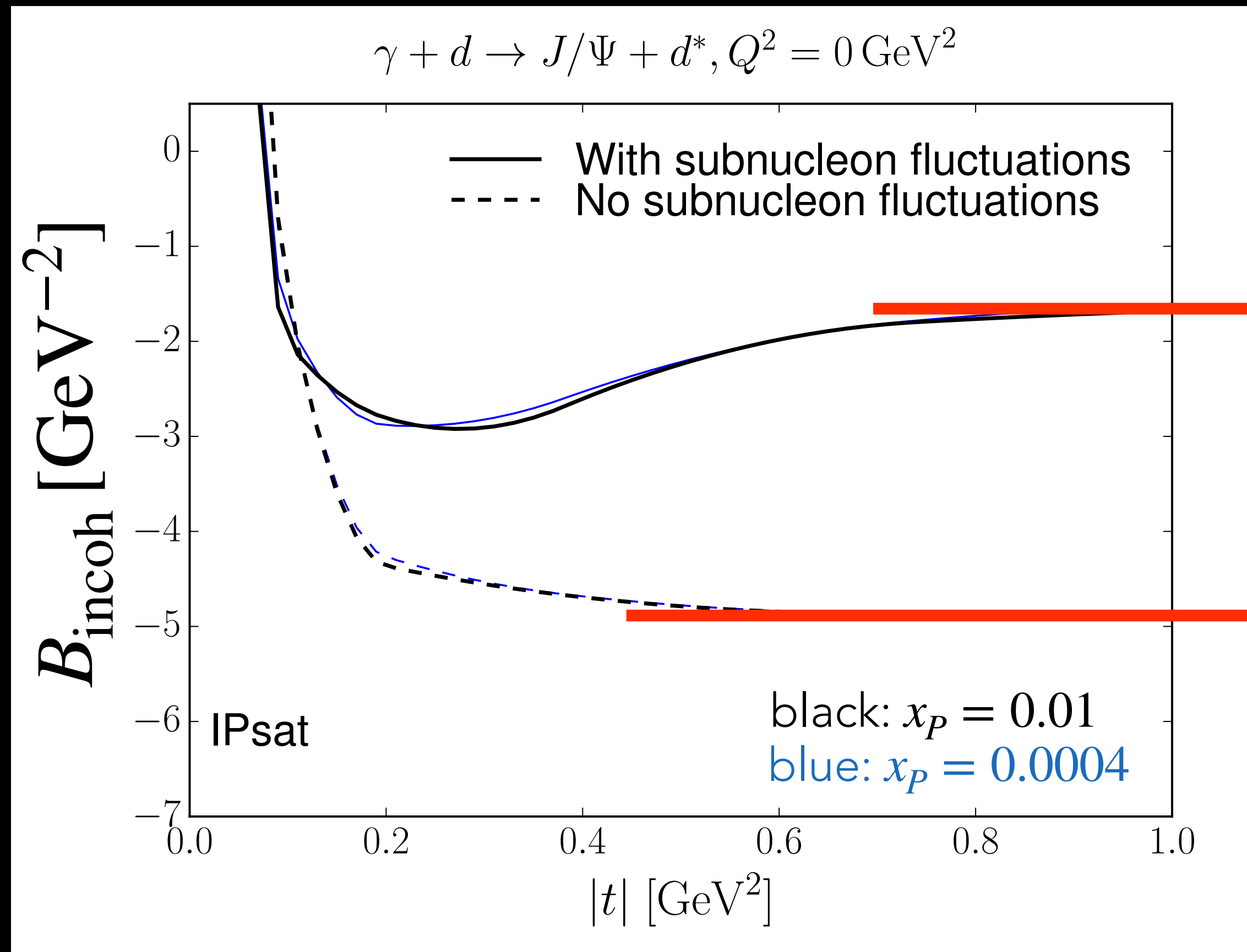


IPSat

Size of fluctuating object controls fall-off of the incoherent xsec $\sim e^{-B_{\text{incoh}}|t|}$
see T. Lappi and H. Mäntysaari, *Phys. Rev. C*83 (2011) 065202

Predictions for the EIC: Slope of incoherent cross section

H. Mäntysaari, B. Schenke, Phys. Rev. C101, 015203 (2020)



IPsat

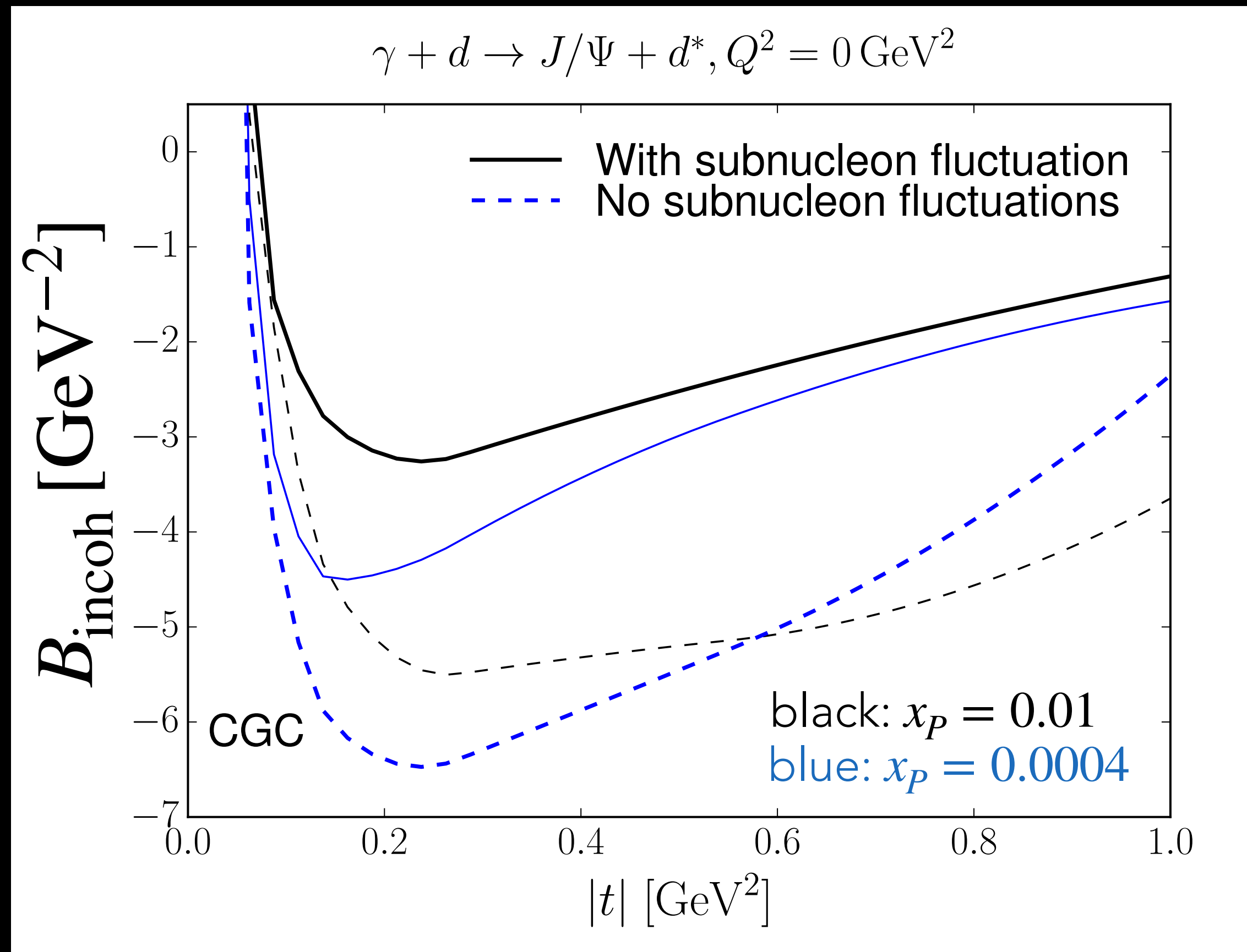
hot spot scale $B_q = 1 \text{ GeV}^{-2}$

nucleon scale $B_p = 4 \text{ GeV}^{-2}$

Size of fluctuating object controls fall-off of the incoherent xsec $\sim e^{B_{\text{incoh}}|t|}$
 see T. Lappi and H. Mäntysaari, Phys. Rev. C83 (2011) 065202

Predictions for the EIC: Slope of incoherent cross section

H. Mäntysaari, B. Schenke, Phys. Rev. C101, 015203 (2020)



CGC

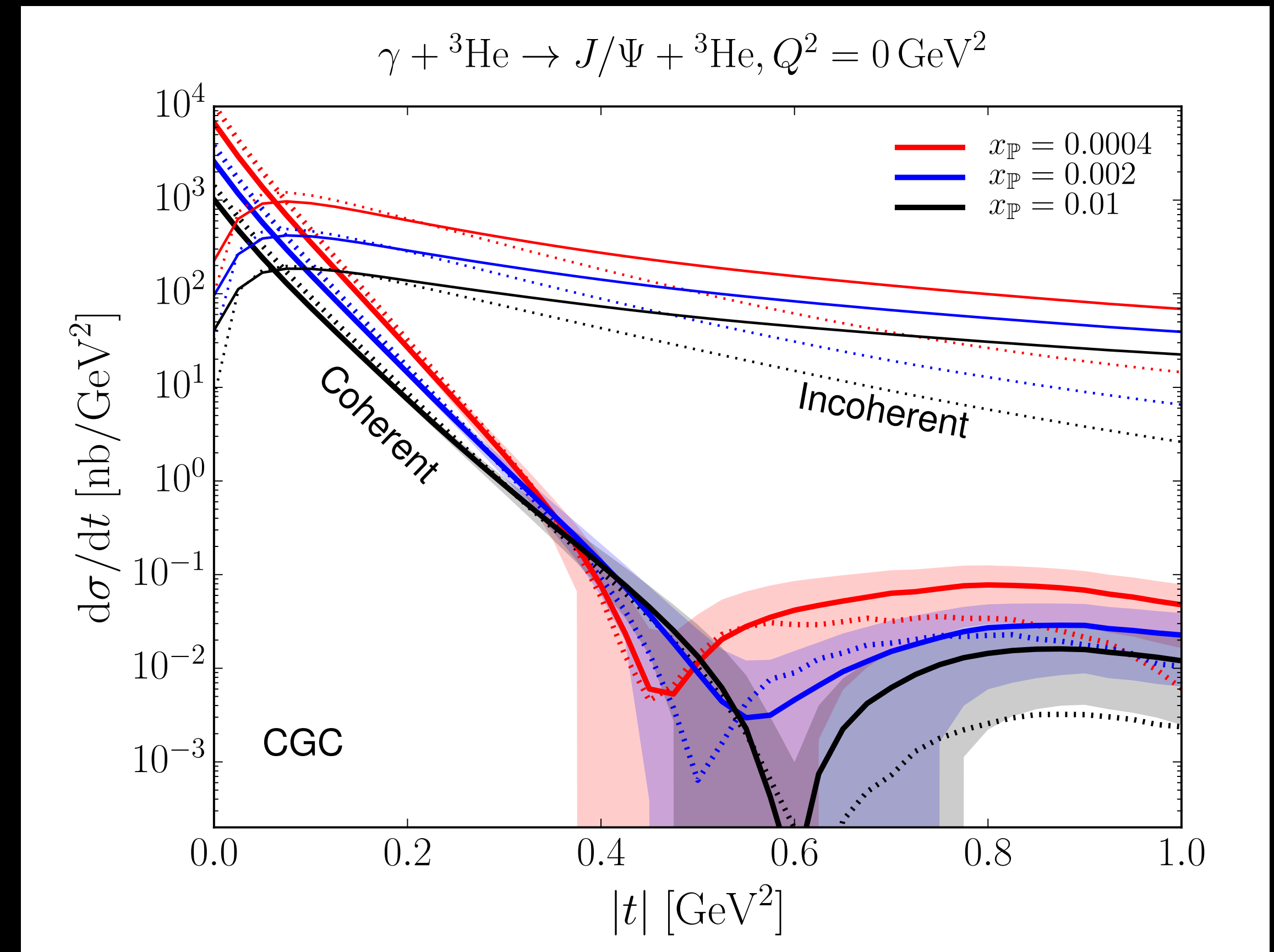
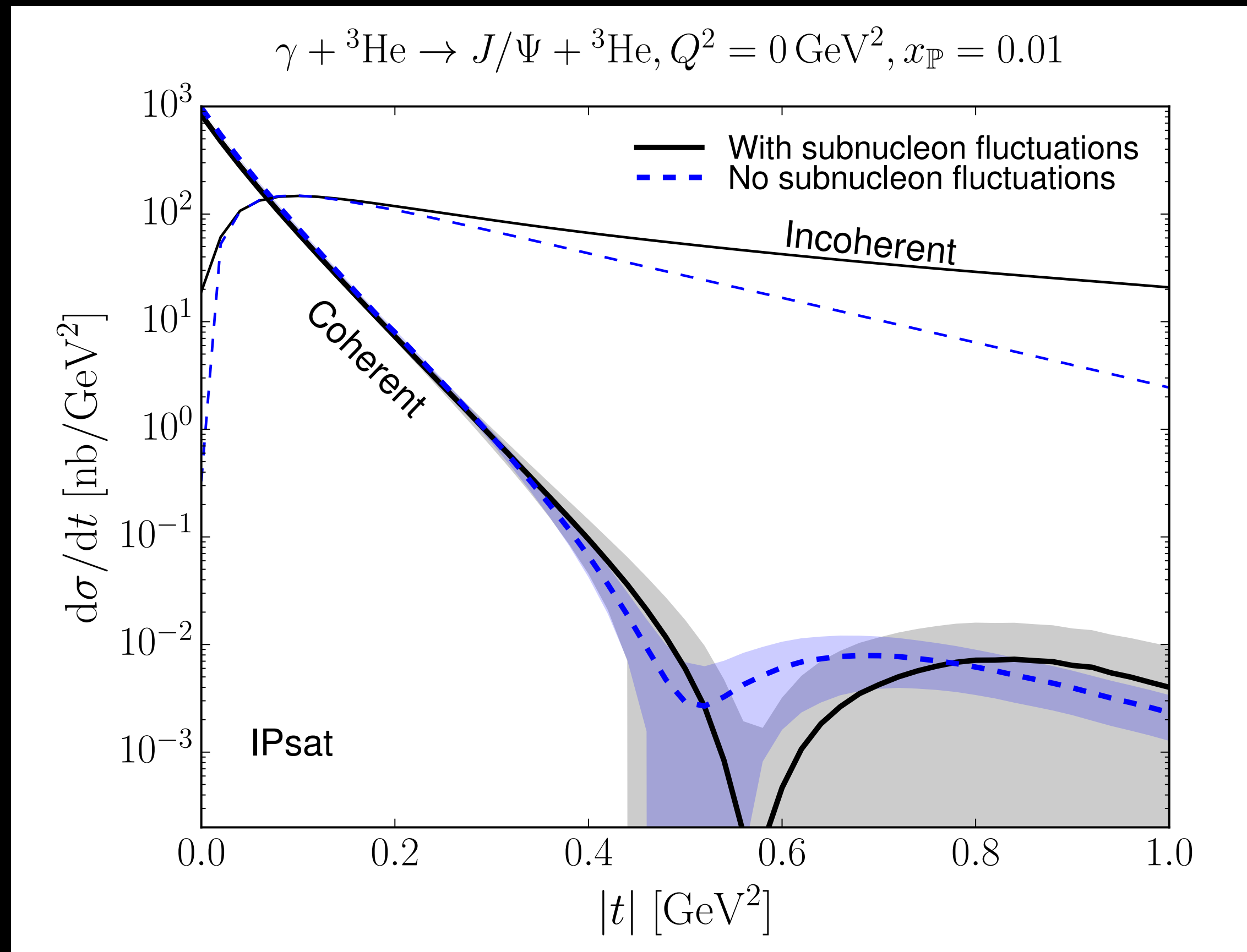
At $|t| \sim 0.2 \text{ GeV}^2$ spectra become steeper with decreasing x (growth of the system and its fluctuating constituents)

Slopes are not constant at large $|t|$
Reason: Color charge fluctuations

At smaller x color charge fluctuations happen on shorter scale $\sim 1/Q_s$ (blue dashed line crosses black dashed line)

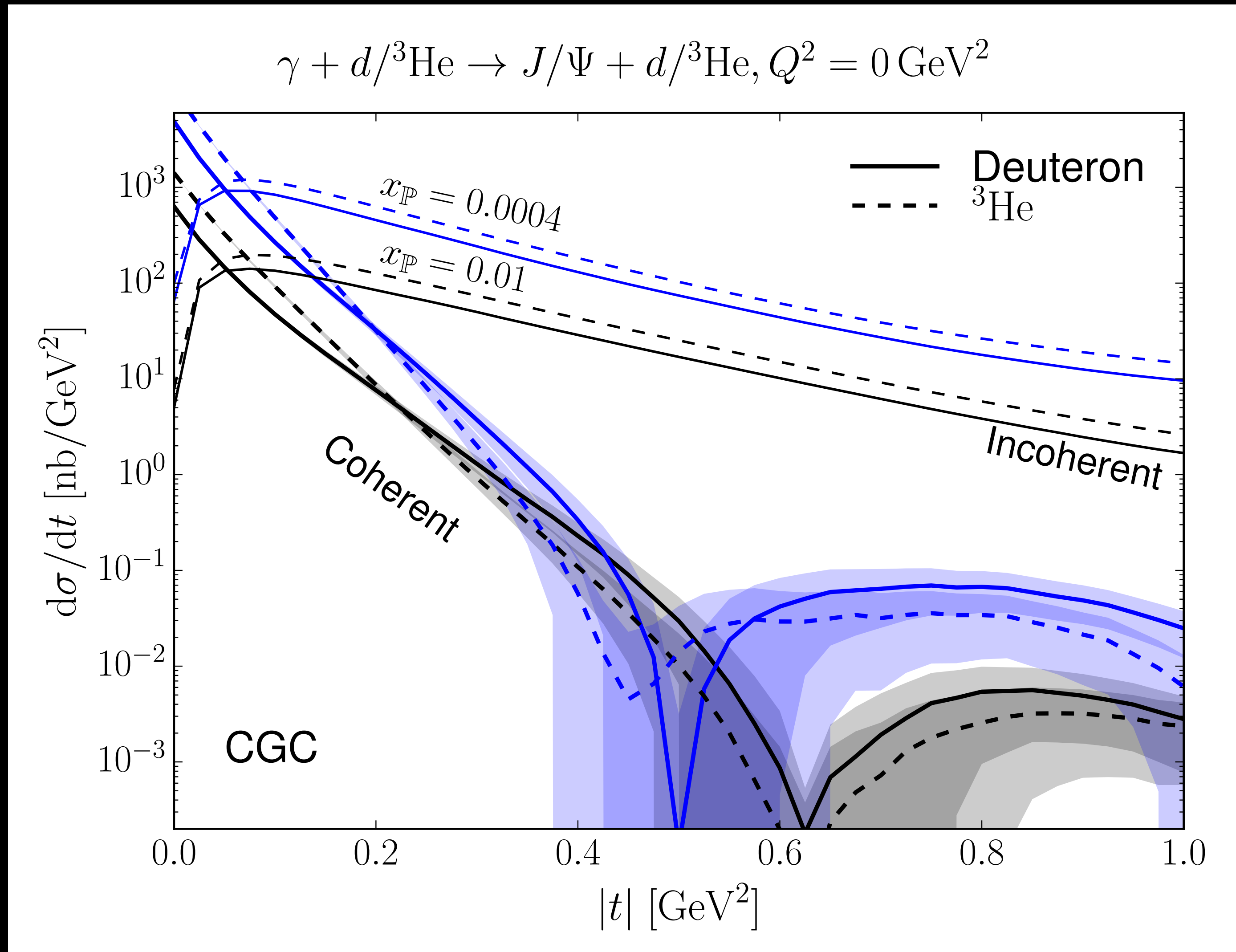
Predictions for the EIC: Cross sections for ^3He targets

H. Mäntysaari, B. Schenke, *Phys. Rev. C*101, 015203 (2020)



Predictions for the EIC: d vs. ^3He targets

H. Mäntysaari, B. Schenke, *Phys. Rev. C*101, 015203 (2020)



Good-Walker/Miettinen-Pumplin

M. L. Good and W. D. Walker, Phys. Rev. 120 (1960) 1857
H. I. Miettinen and J. Pumplin, Phys. Rev. D18 (1978) 1696

Discussing mainly diffractive scattering in p+p collisions, Miettinen and Pumplin ask two questions:

1. What are the states which diagonalize the diffractive part of the S-matrix, so that their interactions are described simply by absorption coefficients?

Answer in their paper: States of the parton model (fixed number N , positions \vec{b}_i , fixed x)

2. What causes the large variations in the absorption coefficients at a given impact parameter, which are implied by the large cross section for diffractive production?

Answer in their paper: Fluctuations in N , \vec{b}_i , x between the states. “Among the parton states which describe a high-energy hadron, there are some which are rich in wee partons, and are therefore likely to interact, while other states have few or no wee partons, and correspond to the transparent channels of diffraction.”

Miettinen-Pumplin: Optical Model Formulation

H. I. Miettinen and J. Pumplin, *Phys. Rev. D*18 (1978) 1696

Target: Average optical potential

Beam particle: $|B\rangle = \sum_k C_k |\psi_k\rangle$ (linear combination of the eigenstates of diffraction $|\psi_k\rangle$)

With $\text{Im}T = 1 - \text{Re}S$ the imaginary part of the scattering amplitude operator, we have

$$\text{Im}T |\psi_k\rangle = t_k |\psi_k\rangle$$

with t_k the probability for eigenstate $|\psi_k\rangle$ to interact with the target (absorption coefficients)

$$\text{Normalize: } \langle B | B \rangle = \sum_k |C_k|^2 = 1$$

$$\text{Elastic scattering: } \langle B | \text{Im}T | B \rangle = \sum_k |C_k|^2 t_k = \langle t \rangle$$

Miettinen-Pumplin: Cross Sections

H. I. Miettinen and J. Pumplin, Phys. Rev. D18 (1978) 1696

Total cross section:

$$d\sigma_{\text{tot}}/d^2\vec{b} = 2\langle t \rangle$$

Elastic cross section:

$$d\sigma_{\text{el}}/d^2\vec{b} = \langle t \rangle^2$$

Incoherent diffractive cross section:

$$\begin{aligned} d\sigma_{\text{diff}}/d^2\vec{b} &= \sum_k |\langle \psi_k | \text{Im}T | B \rangle|^2 - d\sigma_{\text{el}}/d^2\vec{b} = \sum_k |\langle \psi_k | \text{Im}T | \sum_i C_i |\psi_i\rangle|^2 - d\sigma_{\text{el}}/d^2\vec{b} \\ &= \sum_{k,i} |\langle \psi_k | C_i t_i | \psi_i \rangle|^2 - d\sigma_{\text{el}}/d^2\vec{b} = \sum_{k,i} \delta_{ik} |C_i t_i|^2 - d\sigma_{\text{el}}/d^2\vec{b} = \sum_k |C_k|^2 t_k^2 - \langle t \rangle^2 = \langle t^2 \rangle - \langle t \rangle^2 \end{aligned}$$

$$d\sigma_{\text{diff}}/d^2\vec{b} = \langle t^2 \rangle - \langle t \rangle^2$$

Color Glass Condensate calculation

- We study diffractive production in e+p/A (not p+p)
- The projectile can be understood as a quark anti-quark dipole (splitting from the incoming virtual photon)
- The fluctuations are included in the target wave function: Fluctuating spatial distribution of the gluon fields (normalization fluctuations correspond to N fluctuations, spatial fluctuations to \vec{b}_i fluctuations)
(see [Blaizot and Traini, 2209.15545 \[hep-ph\]](#) for the effect of fluctuations of the dipole size)

Fluctuations in the target

Define

$$\hat{T}_p(\vec{b}) = \sum_i^{N_q} T_G(\vec{b}_i - \vec{b}) = \int d^2\vec{x} \hat{\rho}(\vec{x}) T_G(\vec{x} - \vec{b}) \quad T_G \text{ is the gluon distribution in a hot spot}$$

$$\hat{\rho}(\vec{x}) = \sum_i^{N_q} \delta(\vec{x} - \vec{b}_i) \text{ is the hot spot density operator in the transverse plane}$$

The dipole cross section can be written as

$$N = \exp \left[-\frac{1}{2} \sigma_{\text{dip}}(x, \vec{r}) \hat{T}_p(\vec{b}) \right] \approx 1 - \frac{1}{2} \sigma_{\text{dip}}(x, \vec{r}) \hat{T}_p(\vec{b}) \text{ in the weak field limit}$$

$$\text{The dipole cross section then is } \frac{d\sigma_{q\bar{q}}}{d^2\vec{b}} = 2[1 - N] = \sigma_{\text{dip}}(x, \vec{r}) \hat{T}_p(\vec{b})$$

Fluctuations in the target

The dipole cross section then is $\frac{d\sigma_{q\bar{q}}}{d^2\vec{b}} = 2[1 - N] = \sigma_{\text{dip}}(x, \vec{r})\hat{T}_p(\vec{b})$

This operator is diagonal in the basis of states $|\vec{b}_1, \dots, \vec{b}_{N_q}\rangle$, where the \vec{b}_i are the positions of the individual hot spots, frozen during the collision process:

These states can be considered the diffractive eigenstates

Coherent diffractive cross section:

$$\int d^2\vec{b}d^2\vec{b}'e^{-i\vec{\Delta}\cdot(\vec{b}-\vec{b}')} \left\langle \frac{d\sigma^{q\bar{q}}}{d^2\vec{b}} \right\rangle \left\langle \frac{d\sigma^{q\bar{q}}}{d^2\vec{b}'} \right\rangle = \langle \Sigma_{q\bar{q}}(\vec{\Delta}) \rangle^2$$

with $\Sigma_{q\bar{q}}(\vec{\Delta}) = \int d^2\vec{b}e^{-i\vec{\Delta}\cdot\vec{b}}\frac{d\sigma^{q\bar{q}}}{d^2\vec{b}}$ and $\langle \cdot \rangle$ is the average over the ground state wave function

Fluctuations in the target

Total diffractive cross section:

Allow all possible diffractive eigenstates $|\alpha\rangle$ as intermediate states (assume dilute limit here)

$$\int d^2\vec{b} d^2\vec{b}' e^{-i\vec{\Delta}\cdot(\vec{b}-\vec{b}')} \sigma_{\text{dip}}^2 \sum_{\alpha} \left| \langle \alpha | \hat{T}_p(\vec{b}) | \psi_0 \rangle \right|^2 = \langle \Sigma_{q\bar{q}}^2(\vec{\Delta}) \rangle$$

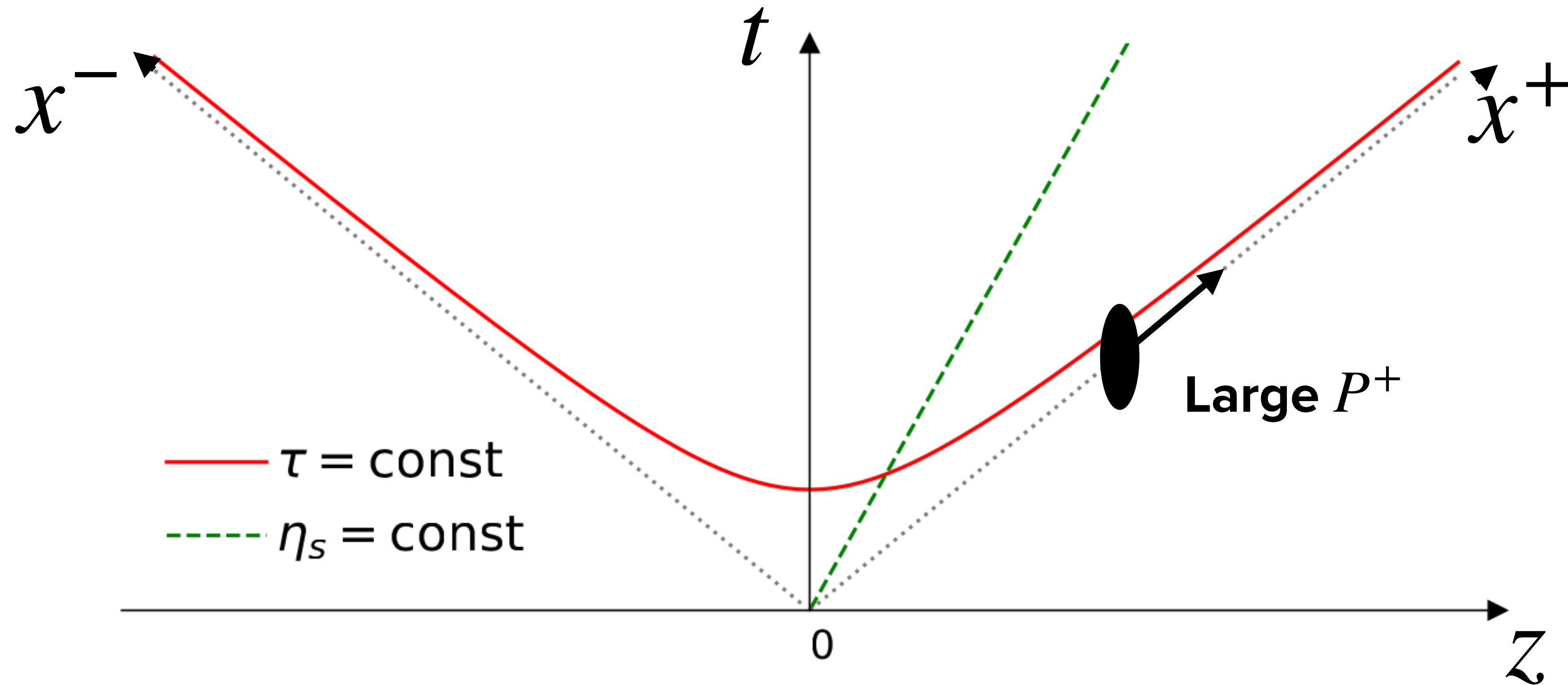
in analogy to the optical model example

This also shows the relation to the density-density correlation function $\langle \hat{T}_p(\vec{b}) \hat{T}_p(\vec{b}') \rangle$

and how we are sensitive to different distance scales via $\vec{b} - \vec{b}'$

See [Blaizot and Traini, 2209.15545 \[hep-ph\]](#) for a more detailed discussion

The scenario: Hadron moving at high momentum



Probe hadron (or nucleus) moving with large P^+ at scale $x_0 P^+$ with $x_0 \ll 1$

Separate partonic content based on longitudinal momentum $k^+ = x P^+$

Large $x > x_0$: Static and localized color sources ρ

Dynamic color fields

The moving color sources generate a current, independent of light cone time z^+ :

$$J^{\mu,a}(z) = \delta^{\mu+} \rho^a(z^-, z_T) \quad a \text{ is the color index of the gluon}$$

This current generates delocalized dynamical fields $A^{\mu,a}(z)$ described by the Yang-Mills equations

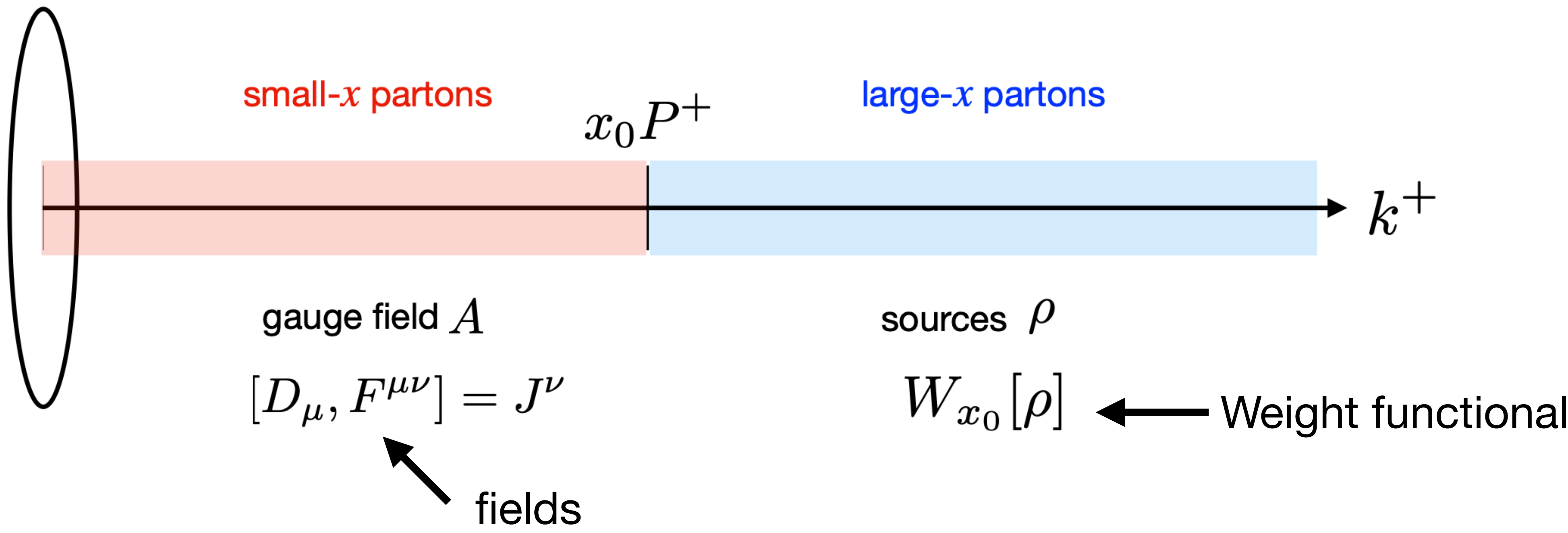
$$[D_\mu, F^{\mu\nu}] = J^\nu$$

with $D_\mu = \partial_\mu + igA_\mu$ and $F_{\mu\nu} = \frac{1}{ig}[D_\mu, D_\nu] = \partial_\mu A_\nu - \partial_\nu A_\mu + ig[A_\mu, A_\nu]$

These fields A are the small $x < x_0$ degrees of freedom

They can be treated classically, because their occupation number is large $\langle AA \rangle \sim 1/\alpha_s$

Color Glass Condensate (CGC): Sources and fields



When $x \lesssim x_0$ the path integral $\langle \mathcal{O} \rangle_\rho$ is dominated by classical solution and we are done

For smaller x we need to do quantum evolution

Wilson lines

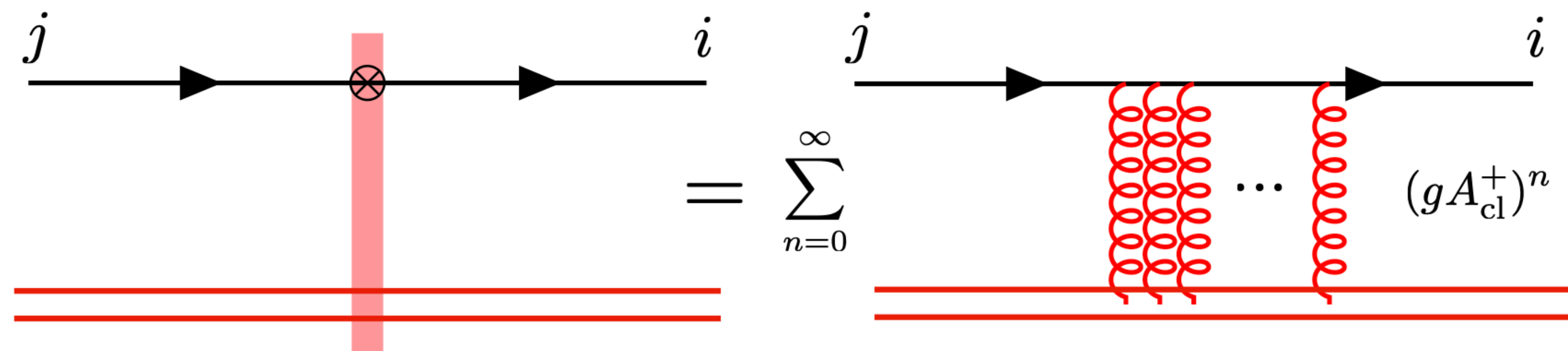
Interaction of high energy color-charged probe with large k^- momentum (and small $k^+ = \frac{k_T^2}{2k^-}$)

with the classical field of a nucleus can be described in the **eikonal approximation**:

The scattering rotates the color, but keeps k^- , transverse position \vec{x}_T , and any other quantum numbers the same.

The color rotation is encoded in a light-like Wilson line, which for a quark probe reads

$$V_{ij}(\vec{x}_T) = \mathcal{P} \left(ig \int_{-\infty}^{\infty} A^{+,c}(z^-, \vec{x}_T) t_{ij}^c dz^- \right)$$



MULTIPLE INTERACTIONS NEED TO BE RESUMMED, BECAUSE $A^+ \sim 1/g$

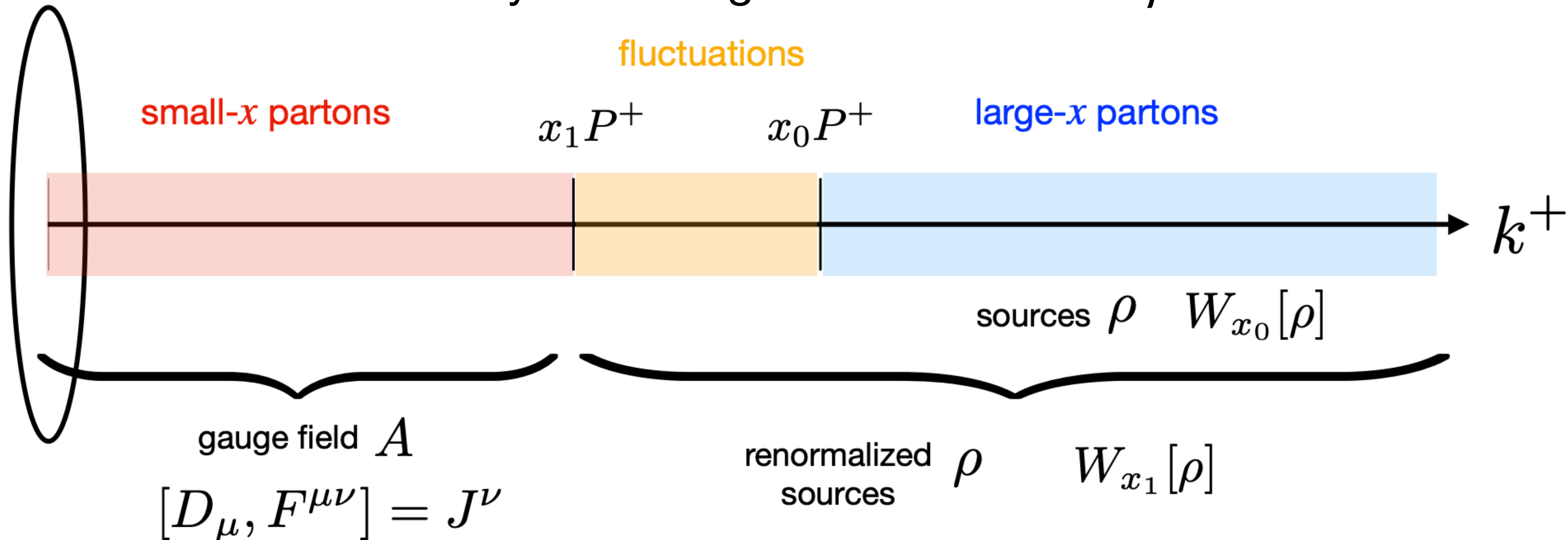
JIMWLK evolution

Jalilian-Marian, J.; Kovner, A.; McLerran, L.D.; Weigert, H., Phys. Rev. D 1997, 55, 5414–5428, [hep-ph/9606337]
 Jalilian-Marian, J.; Kovner, A.; Weigert, H., Phys. Rev. D 1998, 59, 014015, [hep-ph/9709432]
 Kovner, A.; Milhano, J.G.; Weigert, H., Phys. Rev. D 2000, 62, 114005, [hep-ph/0004014]
 Iancu, E.; Leonidov, A.; McLerran, L.D., Nucl. Phys. A 2001, 692, 583–645, [hep-ph/0011241]
 Iancu, E.; Leonidov, A.; McLerran, L.D., Phys. Lett. B 2001, 510, 133–144, [hep-ph/0102009]
 Ferreiro, E.; Iancu, E.; Leonidov, A.; McLerran, L., Nucl. Phys. A 2002, 703, 489–538, [hep-ph/0109115]

LO Small- x evolution resums logarithmically enhanced terms $\sim \alpha_s \ln(x_0/x)$

$$\frac{dW_x[\rho]}{d \ln(1/x)} = - \mathcal{H}_{\text{JIMWLK}} W_x[\rho]$$

Physically, one absorbs the quantum fluctuations in the interval $[x_0 - dx, x_0]$ into stochastic fluctuations of the color sources by redefining the color sources ρ



JIMWLK evolution

Jalilian-Marian, J.; Kovner, A.; McLerran, L.D.; Weigert, H., Phys. Rev. D 1997, 55, 5414–5428, [hep-ph/9606337]
Jalilian-Marian, J.; Kovner, A.; Weigert, H., Phys. Rev. D 1998, 59, 014015, [hep-ph/9709432]
Kovner, A.; Milhano, J.G.; Weigert, H., Phys. Rev. D 2000, 62, 114005, [hep-ph/0004014]
Iancu, E.; Leonidov, A.; McLerran, L.D., Nucl. Phys. A 2001, 692, 583–645, [hep-ph/0011241]
Iancu, E.; Leonidov, A.; McLerran, L.D., Phys. Lett. B 2001, 510, 133–144, [hep-ph/0102009]
Ferreiro, E.; Iancu, E.; Leonidov, A.; McLerran, L., Nucl. Phys. A 2002, 703, 489–538, [hep-ph/0109115]

LO Small- x evolution resums logarithmically enhanced terms $\sim \alpha_s \ln(x_0/x)$

$$\frac{dW_x[\rho]}{d \ln(1/x)} = - \mathcal{H}_{\text{JIMWLK}} W_x[\rho]$$

Physically, one absorbs the quantum fluctuations in the interval $[x_0 - dx, x_0]$ into stochastic fluctuations of the color sources by redefining the color sources ρ

Evolution is done using the Langevin formulation of the JIMWLK equations on the level of Wilson lines

K. Rummukainen and H. Weigert Nucl. Phys. A739 (2004) 183; T. Lappi, H. Mäntysaari, Eur. Phys. J. C73 (2013) 2307

Long distance tails are tamed by imposing a regulator in the JIMWLK kernel, m

S. Schlichting, B. Schenke, Phys.Lett. B739 (2014) 313-319

Isobar shapes - JIMWLK evolution

G. Giacalone, B. Schenke, S. Schlichting, P. Singh, in progress

